AD-A120 840 INFRARED LUMINESCENCE OF CHEMI- AND PHOTON-ACTIVATED MOLECULES(U) MASSACHUSETTS INST OF TECH CAMBRIDGE DEPT OF CHEMISTRY J I STEINFELD 01 SEP 82 AFGL-TR-82-0267 1/1

UNCLASSIFIED F19628-80-C-0028 F/G 7/4 NL

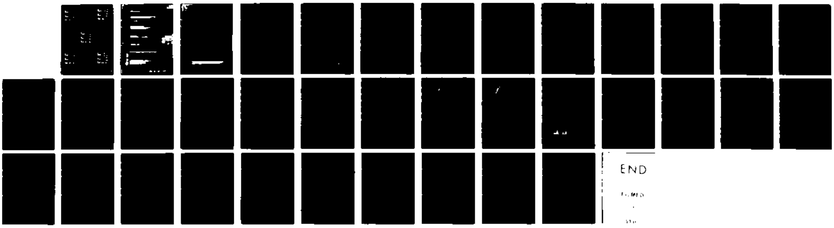

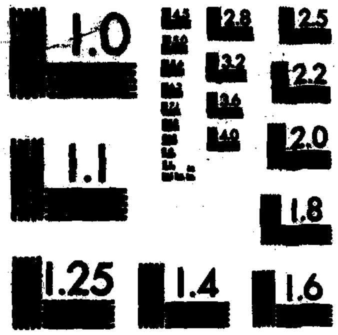
1.0
2.8
2.5
3.2
2.2
3.6
4.0
2.0
1.1
1.8
1.25
1.4
1.6

MICROCOPY RESOLUTION TEST CHART
NATIONAL BUREAU OF STANDARDS-1963-A

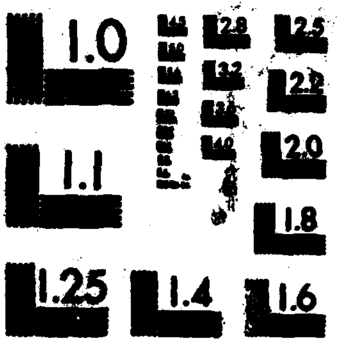
1.0
2.8
2.5
3.2
2.2
3.6
4.0
2.0
1.1
1.8
1.25
1.4
1.6

MICROCOPY RESOLUTION TEST CHART
NATIONAL BUREAU OF STANDARDS-1963-A

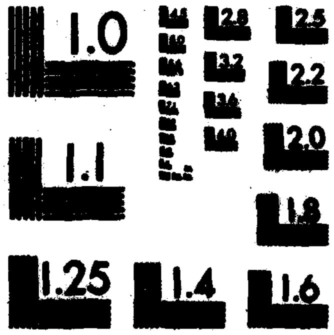
1.0
2.8
2.5
3.2
2.2
3.6
4.0
2.0
1.1
1.8
1.25
1.4
1.6

MICROCOPY RESOLUTION TEST CHART
NATIONAL BUREAU OF STANDARDS-1963-A

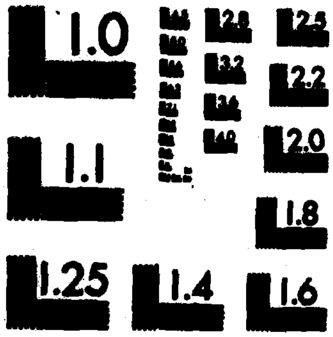
1.0
2.8
2.5
3.2
2.2
3.6
4.0
2.0
1.1
1.8
1.25
1.4
1.6

MICROCOPY RESOLUTION TEST CHART
NATIONAL BUREAU OF STANDARDS-1963-A

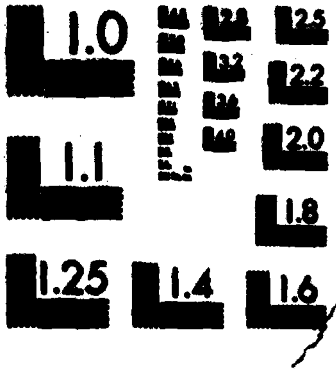
1.0
2.8
2.5
3.2
2.2
3.6
4.0
2.0
1.1
1.8
1.25
1.4
1.6

MICROCOPY RESOLUTION TEST CHART
NATIONAL BUREAU OF STANDARDS-1963-A

ADA120840

REPORT DOCUMENTATION PAGE

READ INSTRUCTIONS BEFORE COMPLETING FORM

1. REPORT NUMBER: AFGL-TR-82-0267

2. GOVT ACCESSION NO.: AD-A120 840

3. RECIPIENT'S CATALOG NUMBER:

4. TITLE (and Subtitle): Infrared Luminescence of Chemi- and Photon-Activated Molecules

5. TYPE OF REPORT & PERIOD COVERED: Final: 01 Nov '79 30 June '82

6. PERFORMING ORG. REPORT NUMBER:

7. AUTHOR(s): J.I. Steinfeld

8. CONTRACT OR GRANT NUMBER(s): F19628-80-C-0028

9. PERFORMING ORGANIZATION NAME AND ADDRESS:
Department of Chemistry
Massachusetts Institute of Technology
Cambridge, Massachusetts 02139

10. PROGRAM ELEMENT, PROJECT, TASK AREA & WORK UNIT NUMBERS:
61102F
2310G4AP

11. CONTROLLING OFFICE NAME AND ADDRESS:
Air Force Geophysics Laboratory
Hanscom AFB, Massachusetts 01731
Monitor/Arthur Corman/OPR

12. REPORT DATE: 01 Sept. '82

13. NUMBER OF PAGES: 36

14. MONITORING AGENCY NAME & ADDRESS (if different from Controlling Office): Same

15. SECURITY CLASS. (of this report): UNCLASSIFIED

15a. DECLASSIFICATION/DOWNGRADING SCHEDULE: N/A

16. DISTRIBUTION STATEMENT (of this Report):

Approved for public release; distribution unlimited

17. DISTRIBUTION STATEMENT (of the abstract entered in Block 20, if different from Report):

18. SUPPLEMENTARY NOTES:

19. KEY WORDS (Continue on reverse side if necessary and identify by block number)

ozone	photoabsorption cross-sections
double resonance	vibrational relaxation
vibrational excitation	reflection principle
Hartley bands	nitrogen

20. ABSTRACT (Continue on reverse side if necessary and identify by block number)

Research ~~has been~~ was performed on the following: (1) vibrational energy tranfer in ozone by infrared-ultraviolet double resonance; (2) sum rules for continuous molecular electronic spectra; (3) ultraviolet continuum spectroscopy of vibrationally excited ozone; (4) Coherent Anti-Stokes Raman detection of ozone in vibrationally excited states; (5) infrared emission and absorption strengths in $^{14}N^{15}N$.

DD FORM 1 JAN 73 1473

Contents

Research Objectives 1

Vibrational Energy Transfer in Ozone by Infrared-Ultraviolet Double Resonance 2
(Chem. Phys. Letts. 76, 479-484 (1980))

Sum Rules for Molecular Electronic Spectra: Application to Exact and Reflection Principle Solutions 8
(Chem. Phys. 64, 421-426 (1982))

Ultraviolet Continuum Spectroscopy of Vibrationally Excited Ozone 14
(J. Chem. Phys. 76, 2201-2209 (1982))

CARS Detection of Ozone in Vibrationally Excited States 23

Infrared Emission and Absorption Strengths for $^{14}N^{15}N$ 27

Publications and Presentations 31

DTIC
COPY
INSPECTED
2

Accession For
NTIS GRA&I ☒
DTIC TAB ☐
Unannounced ☐
Justification
By
Distribution/
Availability Codes
Dist | Avail and/or Special
A

Research Objectives

The goal of this program has been to obtain some or all of the following information regarding highly excited vibrational levels of O_3:

1) Total photon energy uptake in CO_2-laser-pumped O_3; intensity and pressure dependence.

2) Detailed vibrational state populations in multiple-infrared-photon excited O_3.

3) $(v_1 v_2 v_3) \rightarrow (v_1' \ v_2' \ v_3')$ transfer rates as a result of collisions.

4) Spectroscopic description of high ground-state vibrational levels.

5) Vibrational level populations in $O_3{*} \ (^1B_2)$.

6) Hartley band dependence on ground-state vibrational energy content

7) Rotational relaxation times in O_3-M collisions.

8) $(v_1 v_2 v_3)$- dependence of Einstein A and B coefficients for $\Delta v_i = -1$ transitions (i = 1, 2, 3).

Questions (3)-(5) and (8) are applicable to interpretation of the infrared chemiluminescence (COCHISE) experiments: question (6) is applicable to estimation of photodissociation cross-sections for "hot" O_3 in the upper atmosphere.

Experimental approaches have included infrared-ultraviolet double resonance using a pulsed CO_2 laser and a broadband c.w. u.v. source, and Coherent Anti-Stokes Raman detection of ozone in vibrationally excited states.

The results of the i.r.-u.v. double resonance experiments are reported in journal publications reproduced on pp. 2-7 and 14-22; a spectroscopic model for interpreting results will be found on pp. 8-13. Two additional sections describe ongoing CARS experiments on O_3, and an assessment of the contribution of $^{14}N^{15}N$ to upper-atmospheric radiation.

2.

Volume 76, number 3 CHEMICAL PHYSICS LETTERS 15 December 1980

VIBRATIONAL ENERGY TRANSFER IN OZONE BY INFRARED-ULTRAVIOLET DOUBLE RESONANCE

S.M. ADLER-GOLDEN and J.I. STEINFELD
Department of Chemistry, Massachusetts Institute of Technology, Cambridge, Massachusetts 02139, USA

Received 8 September 1980

Absorption transients at 254 nm have been observed in O_3–O_2 mixtures following laser irradiation at 9.64 μm. From analysis of these transients, we are able to determine vibrational relaxation rate constants (O_3–O_2) $\lambda_1^{-1}/[O_2] = (2560 \pm 370)$ Torr^{-1} s^{-1}, $\lambda_2^{-1}/[O_2] = (640 \pm 50)$ Torr^{-1} s^{-1}, and also a υ_1–υ_3 equilibration rate constant (O_3–O_3) of $(1.5 \pm 1.0) \times 10^6$ Torr^{-1} s^{-1}.

1. Introduction

In recent years, a great interest in the study of vibrationally excited ozone has developed, particularly because of its possible role in stratospheric chemistry*. Conveniently, vibrational excitation of the asymmetric stretching mode ν_3 of ozone may readily be induced by CO_2 laser irradiation; multiple-photon excitation and dissociation following such irradiation have recently been reported [2]. Numerous studies using laser excitation have been carried out to determine the kinetics of vibrational energy flow in ozone and quenching by various collision partners. Most of the kinetic information to date has been obtained by either infrared fluorescence [3-6] or by an indirect method based on the chemiluminescent reaction of vibrationally excited ozone with NO [7-9]. Recently, a new technique has been reported [10] using time-resolved ultraviolet absorption spectroscopy at 310 nm following CO_2 laser irradiation (IRUVDR). It was pointed out that the inherent advantages of IRUVDR are high signal-to-noise ratios and fast time response. However, the rate constants obtained in that study were not unambiguously interpretable and in some cases were of low precision.

In this paper we report an IRUVDR experiment at 254 nm (near the peak of the Hartley continuum) which yields rate constants for *all* of the energy transfer processes in ozone, namely,

$$O_3^*(001) + M \underset{k_{13}}{\overset{k_{31}}{\rightleftharpoons}} O_3^*(100) + M\,, \tag{1}$$

$$\left.\begin{matrix} O_3^*(001) \\ O_3^*(100) \end{matrix}\right\} + M \underset{k_{-1}}{\overset{k_1}{\rightleftharpoons}} O_3^*(010) + M\,, \tag{2}$$

and

$$O_3^*(010) + M \xrightarrow{k_2} O_3(000) + M\,, \tag{3}$$

where $M = O_3$ or an added buffer gas and the k refer to first-order rate constants. The buffer gas used in this study was oxygen, both for convenience and because the literature is most extensive for $M = O_2$ [3, 5, 7, 8]. Values of the second-order rate constants for O_3–O_2 collisions, $k_i^{O_3-O_2}/[O_2]$, were obtained for processes (2) and (3) and were found to display both high precision and good agreement with previous literature values. The current work, while not of sufficient precision to permit more than rough estimates of the rate constants in (1), does represent the first reported observation of that kinetic process.

The rationale for using UV absorption spectroscopy to probe vibrational energy content in ozone has been discussed by McDade and McGrath [10]; in essence, vibrational excitation leads to a change in the extinction coefficient at a given wavelength. The absorption spectrum of a particular vibrational level is as yet unknown, although a spectral analysis has been conjectured by Simons and others [12, 13], based on the temperature dependence of the Hartley continuum absorbance. Two points do seem clear: firstly, the (010) level has the same or nearly the same extinction coefficient as ground-state ozone, particularly at the peak of the spectrum near 254 nm; secondly, the combined (100) and (001) levels (roughly equal in population at and above room temperature) have a much broader spectrum, hence a greatly decreased extinction coefficient at 254 nm compared to ground-state ozone. Thus, the expectation is that CO_2 laser irradiation induces a transient decrease in the absorbance at 254 nm, roughly in proportion to the combined (100) and (001) level populations, which are assumed to be in thermal equilibrium shortly after the laser pulse. This prediction has been borne out by the current experiments. A contribution to the transient which arises from translational heating has been observed by McDade and McGrath [10]; we also observed this effect in ozone-oxygen samples containing more than 10% ozone. To simplify our rate constant measurements we confined ourselves to more dilute mixtures.

---

* For a recent review of ozone photochemistry and spectroscopy, see ref. [1].

2. Experimental

A schematic diagram of the apparatus is shown in fig. 1. The IR/UV absorption cell was a pyrex cylinder 20 cm long and 2.5 cm wide fitted with NaCl end windows and UV-grade quartz side windows through which the UV beam was passed transverse to the IR beam. The cell was filled with a static sample of from 5 to 50 Torr of a 1% to 10% mixture of ozone in oxygen. The ozone was prepared from a silent discharge ozonizer and stored on a silica gel trap at 195 K. The oxygen diluent also derived from the cold trap and thus was free of moisture. The total pressure in the cell was measured by a U-tube manometer filled with Halocarbon 100/100 oil, and the ozone concentration was monitored by UV absorption. The UV source was a Heath EU-701-50 deuterium lamp fitted with a 253.7 nm interference filter. The IR pulse was provided by a Tachisto Tac II TEA CO_2 laser operating on the 10^00–02^00 P(30) line, giving typically 0.4 J in a duration of ≈ 100 ns (fwhm).

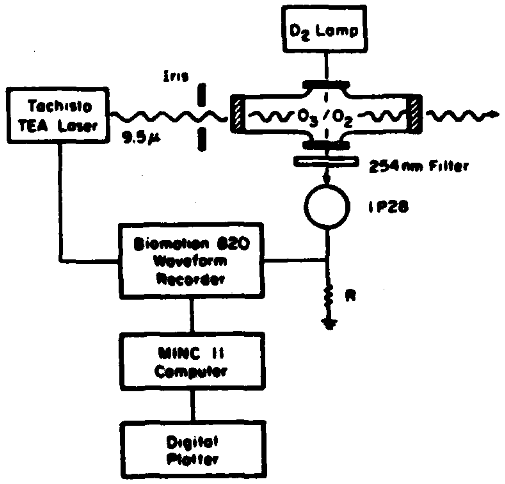

Fig. 1. Schematic diagram of experimental apparatus.

The output from the photomultiplier tube (RCA 1P28) was fed across a variable resistance (≈1 kΩ) to a Biomation 820 waveform recorder interfaced to a Digital MINC-11 computer which performed signal averaging, display, and analysis*. Typically 50 to 200 laser pulses were averaged per data point. The time response of the electronics was estimated to be 0.2 μs. Signal analysis was accomplished by digital smoothing followed by a non-linear least-squares fitting procedure.

3. Results and discussion

Typical CO_2 laser-induced absorbance transients are shown in figs. 2a and 2b. In fig. 2a the transient reaches a maximum value after an "induction time" ($t_{\max}$) of about 3 μs and then decays according to the time evolution of the combined (100) and (001) level populations, described by a double-exponential function [3]. The solid curve is a 3-parameter least-squares fit to that function. In fig. 2b, taken at lower pressures of O_2 and O_3, the "induction time" is about 9 μs, indicating that it arises from a kinetic

---

* A description of the transient recorder–computer interface may be found in ref. [13].

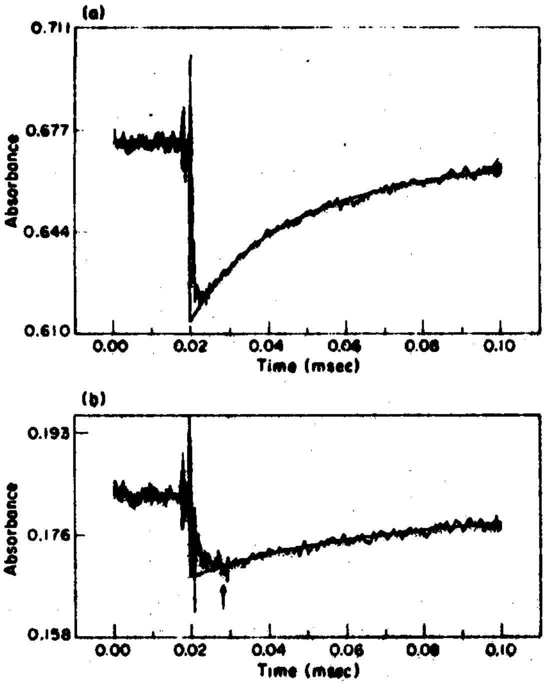

Fig. 2. Typical laser-induced absorbance transients in ozone at 254 nm. (a) Experimental and calculated transients at $[O_2] = 29.5$ Torr, $[O_3] = 0.54$ Torr, showing double exponential decay. (b) Experimental and calculated transients at $[O_2] = 12.9$ Torr, $[O_3] = 0.15$ Torr, showing "induction time" t_{ind} denoted by arrow. In both traces the decaying portion was digitally smoothed.

process rather than an instrumental effect. We presume this process to be the fast $\nu_1 \rightleftarrows \nu_3$ equilibration step.

The first-order rate constants k_1 and k_2 were determined from selected traces such as in fig. 2a where the signal-to-noise ratio was good enough and the observation time was sufficiently long that both components of the decay were well determined. The main contribution to the observed rates is due to O_3–O_2 collisions under our experimental conditions. Thus, we were able to obtain O_3–O_2 second-order (bimolecular) rate constants, $k_i^{O_3-O_2}/[O_2]$, by subtracting from the first-order rate constants and contributions arising from O_3–O_3 collisions, as calculated from literature rate constants [4]. It was assumed that at the total pressures used the influence of both diffusion and spontaneous radiative decay may be neglected.

Two quantities which are related to the first-order rate constant k_1 and k_2 are λ_1^{-1} and λ_2^{-1}, the inverse lifetimes associated with the two exponential decay components; the relationships between these quantities are given by Rosen and Cool [3]. Correspondingly related to the second-order rate constants are the second-order inverse lifetimes $(\lambda_1^{O_3-O_2})^{-1}/[O_2]$ and $(\lambda_2^{O_3-O_2})^{-1}/[O_2]$; these are the constants which have been the most commonly measured by other workers. We computed these second-order inverse lifetimes for each data point from the second-order rate constants determined above.

It was found that, using the above analysis, a systematic error appeared in the second-order constants, namely, a slight decrease (≈20%) at high total pressures (30–50 Torr). As high pressures are correlated with high degrees of laser excitation, we presume that the problem is caused by the population of vibrational levels having $v > 1$. The kinetic equation must be corrected to account for vibrational energy contained in those high-lying levels and the effect of those levels on the extinction coefficient at 254 nm must be estimated. The first correction consists merely of the replacment of excited ozone population by total excess vibrational energy contained in the ν_1 and ν_3 manifolds [3, 14]. The second correction is not readily determined as it involves knowledge of the Hartley continuum spectroscopy of high v levels. However, a semi-empirical approach is available. Simons and others [11, 12] have modeled the Hartley continuum using a quasi-diatomic picture in which the spectrum depends mainly on the vibrational energy contained in the ν_1 manifold. The temperature dependence of the absorbance maximum of a diatomic molecule is described rather well by the Sulzer–Wieland equation [15, 16],

$$A_T = A_0[(\bar{E}_v)_0/(\bar{E}_v)_T]^{1/2}, \tag{4}$$

where $(\bar{E}_v)_T$ is the mean vibrational energy including zero point energy at temperature T and A_T is the absorbance at that temperature. To apply this equation to ozone, $\bar{E}_v$ must be understood as the average energy contained in the ν_1 manifold or, alternatively, the roughly equal quantities of energy contained in either ν_3 or the hypothetical mode $\bar{\nu} = (\nu_1 + \nu_3)/2$ defined by Rosen and Cool [3]. We have used eq. (4), with the approximation of the doubly degenerate mode $\bar{\nu}$ as defined above, for an improved analysis of our data. Our results (table 1 and fig. 3) show that this method of analysis does indeed remove the systematic rate constant error described above, as evidenced by the absence of any pressure dependence of the second-order inverse lifetimes (fig. 3).

It must be cautioned, however, that the observed empirical success of the Sulzer–Wieland equation as applied to ozone in no way implies the correctness of the quasi-diatomic spectral model. We are currently carrying out a more accurate treatment of the ozone spectrum [17] based on both wavelength-dependent experiments and ab initio calculations [18]. Preliminary indications are that the quasi-diatomic model is substantially incorrect.

The current values for the O_3–O_2 bimolecular rate constants and inverse lifetimes may be compared to previous literature values (table 1). Our value of $(\lambda_2^{O_3-O_2})^{-1}/[O_2]$ agrees excellently with the determination via IR fluorescence by Rosen and Cool [3], but is substantially larger than values obtained by Kurylo et al. [7] and West et al. [5]. However, it has been pointed out that the NO chemiluminescence technique used by Kurylo systematically underestimates the true decay constant λ_2^{-1}, especially for low values of $\alpha = k_1/k_2$ [9]. Using our current α value of 1.6 one expects about a 25% error in Kurylo's measurement. There is also reason to believe that the West [5] measurements of both λ_2^{-1} and λ_1^{-1} via IR fluorescence are also too low, as their analysis relied on an approximation valid only in the limit of high laser excitation [3], a condition which was not experimentally verified and which becomes progressively inaccurate as the decay proceeds to longer times.

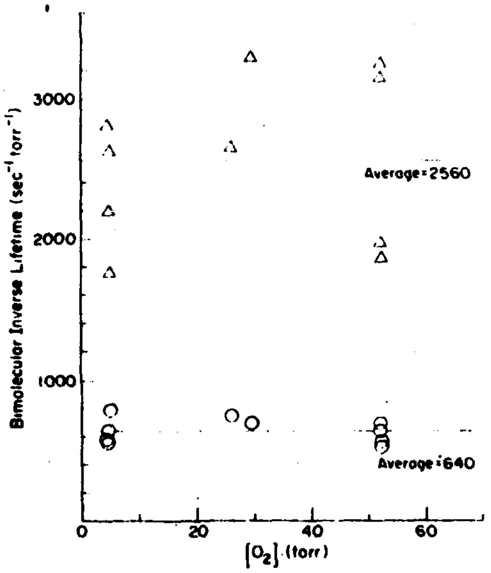

Fig. 3. bimolecular inverse lifetimes $\lambda_1^{O_3-O_2}/[O_2]$ and $\lambda_2^{O_3-O_2}/[O_2]$, denoted by ○ and △, respectively.

Table 1
Comparison of values for the O_3–O_2 second-order rate constants and inverse lifetimes ($Torr^{-1} s^{-1}$)

	This work[a]	Rosen and Cool [3]	Kurylo et al. [7]	West et al. [5]
$k_1/[O_2]$	1670±370	–	–	1200±600
$k_2/[O_2]$	990±110	–	–	650±200
$\lambda_1/[O_2]$	2560±370	–	–	1810±450[b]
$\lambda_1/[O_2]$	640±50	625±125	425±40	430±110[b]

[a] Errors are 95% confidence limits.
[b] From published values of $k_1/[O_2]$ and $k_2/[O_2]$.

The accurate determination of k_{13} and k_{31} from the initial portion of the transient (see fig. 2b) was hampered by the poor signal-to-noise ratio at short time scales and by rf interference caused by the laser. The expected shape of the transient would consist of a nearly instantaneous absorbance change associated with the laser-induced population of the (001) state, followed by a second absorbance change occurring over several microseconds which would be associated with energy transfer to other levels within the ν_1 and ν_3 manifolds, principally (100), until equilibrium within these manifolds is established. The observed traces (fig. 2) are consistent with this model as far as can be determined. The magnitude of the instantaneous absorbance change is masked by the laser noise but it is certainly smaller than the maximum absolute value of the transient, since absorbance decreases as the $\nu_1 \rightleftharpoons \nu_3$ equilibration proceeds. An immediate conclusion which may be drawn is that at 254 nm the (100) state is more transparent than the (001) state.

Given the poor quality of the data we have not attempted to fully model the transient. Instead, we have roughly estimated the first-order constants k_{13} and k_{31} by measuring the "induction time" after the pulse, t_{max}, at which the transient reaches its maximum absolute value. By that time, the experimental traces are free from laser interference. Assuming the model described by (1) and (2) (using equal rate constants k_1 for deactivation of both stretching modes) it may be shown that

$$(k_{13}+k_{31}+k_1)\exp[-(k_{13}+k_{31})t_{max}] = [(0.37R+0.85)/(0.85-R)]k_1 , \qquad (5)$$

where $R = \Delta A_{001}/\Delta A_{100}$, the ratio of absorbance transients pertaining to the (001) and (100) excited ozone. R is also related to the ratio of the instantaneous transient ($t = 0$) to the transient at t_{max}. The laser interference precludes the determination of R, although we may estimate $0 < R < 0.4$ from the previous discussion. With $R = 0$ eq. (5) [illegible] steady-state condition for [illegible].

From the experimental traces and eq. (5) we estimate a value for $(k_{13}+k_{31})^{O_3-O_2}/[O_2]$ of [illegible] $\times 10^{5}$ Torr^{-1} s^{-1}; it is relatively insensitive to the value of R chosen. This is consistent with the [illegible] of 1.6×10^{5} Torr^{-1} s^{-1} [illegible] [3], and with their [illegible] V–V coupling processes [illegible] occurring in one in every [illegible] collisions. Our [illegible] value for $(k_{13}+k_{31})$[illegible] $(1.1 \pm 0.5) \times$ 10^{6} Torr^{-1} s^{-1}. [illegible] more accurate data. From the present work, it may certainly be concluded that ozone is a [illegible] efficient promoter of [illegible] coupling than oxygen, presumably [illegible] the coupling proceeds via a resonant exchange mechanism.

Finally, in the [illegible] experiments, eq. (4) relates the absorbance to the vibrational energy content, an approximate value for the mean number of CO_2 photons deposited per ozone molecule may be obtained. With a laser fluence of roughly 100 mJ/cm^2 we estimate an average of around 0.1 photons/molecule at low total pressure (around 5 Torr), which increases to about 0.5 photons/molecule in the pressure range of 30–50 Torr. For comparison, Zittel and Little [19] found that 0.6 photons/molecule were deposited at 20 Torr with a comparable fluence.

As mentioned previously, multiphoton excitation and dissociation of ozone has been reported using a more powerful CO_2 laser and a focused beam [2]. A transient decrease in the UV absorption at 270 nm was observed following laser irradiation of an ozone–oxygen mixture, and a permanent decrease in absorption was also found after a number of laser pulses. From the current estimates of the rate constants for $\nu_1 \rightleftharpoons \nu_3$ energy transfer, the value of $k_{13}+k_{31}$ is on the order of 7×10^{5} s^{-1} for the gas mixture used, and that is compatible with the observed rise time of the UV transient. We therefore suggest that the observed transient may be associated with the $\nu_1 \rightleftharpoons \nu_3$ energy transfer process. The identification of the transient as resulting from ozone dissociation is thus open to question, as a similar transient occurring in the absence of dissociation was observed in the current work.

6. Conclusions

The IRUVDR technique has been shown to provide a [illegible] means for the measurement of accurate rate constants for vibrational energy transfer in ozone. It is the only method currently available which is capable of providing information on all three of the [illegible] processes, including the hitherto [illegible] near-resonant $\nu_1 \rightleftharpoons \nu_3$ process. Further experiments will allow the more precise determination of the $\nu_1 \rightleftharpoons \nu_3$ rate constants as well as values for the extinction coefficient as a function of vibrational excitation in the ν_1 and ν_3 manifolds. The latter information, if determined over a suitable range of wavelengths, should enable the deduction of the shape of the potential surface upon which the Hartley transition terminates.

Acknowledgement

This work was supported by the Air Force Geophysics Laboratory, Contract No. F19628-80-C-0028.

References

[1] H. Okabe, Photochemistry of small molecules (Wiley, New York, 1978).

[2] D. Proch and H. Schröder, Chem. Phys. Letters 61 (1979) 426.
[3] D.I. Rosen and T.A. Cool, J. Chem. Phys. 62 (1975) 466.
[4] K.-K. Hui, D.I. Rosen and T.A. Cool, Chem. Phys. Letters 32 (1975) 141.
[5] G.A. West, R.E. Weston Jr. and G.W. Flynn, Chem. Phys. Letters 42 (1976) 488.
[6] G.A. West, R.E. Weston Jr. and G.W. Flynn, Chem. Phys. Letters 56 (1978) 429.
[7] M.J. Kurylo, W. Braun and A. Kaldor, Chem. Phys. Letters 27 (1974) 249.
[8] R.J. Gordon and M.C. Lin, J. Chem. Phys. 64 (1976) 1058.
[9] J. Moy, C.-R. Mao and R.J. Gordon, J. Chem. Phys. 72 (1980) 4216.
[10] I.C. McDade and W.D. McGrath, Chem. Phys. Letters 72 (1980) 432.
[11] J.W. Simons, R.J. Paur, H.A. Webster III and E.J. Bair, J. Chem. Phys. 59 (1973) 1203.
[12] T. Kleindienst and E.J. Bair, Chem. Phys. Letters 49 (1977) 338;
T. Kleindienst, J.B. Burkholder and E.J. Bair, Chem. Phys. Letters 70 (1980) 117.
[13] C. Reiser, Rev. Sci. Instr., to be published.
[14] R.N. Schwartz, Z.I. Slawsky and K.F. Herzfeld, J. Chem. Phys. 20 (1952) 1591.
[15] P. Sulzer and K. Wieland, Helv. Phys. Acta 25 (1952) 653.
[16] R.J. Leroy, R.G. MacDonald and G. Burns, J. Chem. Phys. 65 (1976) 1485.
[17] S.M. Adler-Golden and J.I. Steinfeld, to be published.
[18] P.J. Hay and T.H. Dunning, J. Chem. Phys. 67 (1977) 2290.
[19] P.F. Zittel and D.D. Little, J. Chem. Phys. 72 (1980) 5900.

Chemical Physics 64 (1982) 421–426
North-Holland Publishing Company

SUM RULES FOR MOLECULAR ELECTRONIC SPECTRA: APPLICATION TO EXACT AND REFLECTION PRINCIPLE SOLUTIONS

S.M. ADLER-GOLDEN
Department of Chemistry, Massachusetts Institute of Technology,
Cambridge, Massachusetts 02139, USA

Received 13 July 1981

Sum rules for overlap integrals are presented which give the width and mean frequency of an electronic spectrum as a function of potential curves and internal energy. Exact quantum mechanical results are compared with both the tradditional reflection principle and a modification of it which conserves momentum. Applications to real spectra, particularly continuous absorption spectra of small molecules, are discussed.

1. Introduction

The intensity distribution in molecular electronic spectra is generally given by the Franck–Condon integral, the evaluation of which is sufficiently inconvenient that approximation methods and qualitative arguments are often invoked. As a first approximation, one frequently assumes a constant electronic transition moment, reducing the problem to the computation of the squared overlap integral, $|\langle\psi_f|\psi_i\rangle|^2$ [1], where ψ_i and ψ_f denote initial and final rovibrational wavefunctions. A second, more drastic approximation, such as the "reflection principle" ("delta function approximation") [2,3] is often used to evaluate the overlap integral. Qualitative arguments have been derived from the reflection principle, as, for example, the commonly held but false assumption that enhancement of vibrational energy necessarily red-shifts an absorption spectrum and blue-shifts an emission spectrum [4–6].

Ideally, principles by which electronic spectra are analyzed should derive from exact quantum mechanics rather than approximations. In this paper sum rules for overlap integrals are presented which yield exact quantum mechanical expressions for the width and mean frequency of an electronic spectrum without requiring the actual computation of the overlap integrals. Previous work in this area [5] relied on the reflection principle, which led to incorrect results. In addition, exact and approximate expressions for the overlap integral, including two distinct forms of the reflection principle, are compared via the sum rules, and applications of the theory to experimental spectra are discussed.

2. Diatomic molecules

Let $V_f(q)$ and $V_i(q)$ denote final and initial effective potential functions of coordinate q, and define $\Delta V = V_f(q) - V_i(q)$. Define

$$\langle(h\nu)^n\rangle = \sum_f |\langle\psi_f|\psi_i\rangle|^2 (h\nu)^n ,$$

namely, the mean or expectation value of $(h\nu)^n$ for the electronic spectrum arising from the rovibrational level i. (To compute the mean from a spectrum, the intensity must be converted to an overlap integral squared by dividing by an appropriate power of $(h\nu)$, and by assuming a constant transition moment [1].) The sum rules are:

$$\langle(h\nu)^n\rangle = \langle\psi_i|(\Delta V)^n|\psi_i\rangle \qquad n = 1, 2 \text{ only.} \qquad (1)$$

For shorthand we may denote the right hand side as $\langle(\Delta V)^n\rangle$. The proofs derive from elementary operator

0301-0104/82/0000–0000/$ 02.75 © 1982 North-Holland

The U.S. Government is authorized to reproduce and sell this report. Permission for further reproduction by others must be obtained from the copyright owner.

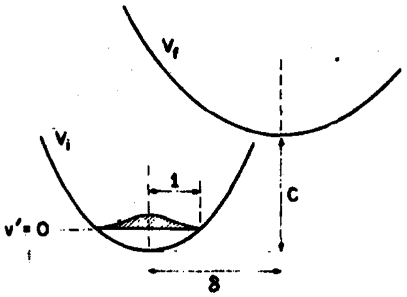

Fig. 1. Model potentials, $V_i = q^2/2$, $V_f = (\omega_f/\omega_i)^2(q-\delta)^2/2 + C$. Energy and distance are dimensionless (energy is in units of $\hbar\omega_i$).

algebra (see appendix), yet the existence of these identities appears to be unknown to the general spectroscopic literature.

Eq. (1) yields both the mean frequency, $\langle h\nu\rangle$, and the variance, $\sigma^2 = \langle (h\nu)^2\rangle - \langle h\nu\rangle^2$, of the spectrum. The quantities on the right hand side are readily evaluated matrix elements. For example, with harmonic oscillator potentials (refer to fig. 1 for definitions of δ and C) the results are

$$(\hbar\omega_i)^{-1}\langle h\nu\rangle = \tfrac{1}{2}E_i(R-1) + R\delta^2/2 + C, \tag{2a}$$

$$\begin{aligned}(\hbar\omega_i)^{-2}\langle (h\nu)^2\rangle &= (R\delta^2/2 + C)^2 \\ &+ E_i[(R-1)(R\delta^2/2 + C) + (R\delta)^2] \\ &+ \tfrac{3}{8}(E_i^2 + \tfrac{1}{4})(R-1)^2,\end{aligned} \tag{2b}$$

where $E_i = v' + 1/2$, the initial vibrational energy in dimensionless units, and $R = (\omega_f/\omega_i)^2$, the ratio of curvatures in the final and initial states; ω_f and ω_i are the corresponding vibrational frequencies.

3. Qualitative aspects

Several conclusions are readily apparent from eqs. (2a) and (2b) regarding the influence of internal energy on a spectrum. It is seen from (2) that vibrational energy in the initial state affects the mean frequency according to the relationship between the ground and excited state curvatures. If $\omega_i = \omega_f$ the mean frequency is invariant. However, vibrational excitation always increases the width of a spectrum. Isotopic substitution will affect the shape of the spectrum by changing the vibrational energy content, essentially by altering the zero point energy. Rotational energy plays a somewhat different role. In the Q branch approximation ($\Delta J = 0$), which works quite well for diffuse spectra, ΔV is unaffected by rotational energy, as the same centrifugal terms appear in both effective potentials, V_f and V_i. However, $\psi_i(q)$ is shifted to a longer distance, thus $\langle h\nu\rangle$ will shift according to the behavior of ΔV at that distance.

The sum rules are most useful for continuous, bound-free spectra, where the lack of vibronic structure precludes a conventional analysis. We must replace the sum by an integral in the definition of $\langle (h\nu)^n\rangle$; i.e.,

$$\langle (h\nu)^n\rangle = \int |\langle\psi_f|\psi_i\rangle|^2 (h\nu)^n \, \mathrm{d}E_f,$$

where E_f is the (continuous) final state energy and the final state wavefunctions are appropriately normalized. Eqs. (2a) and (2b) for harmonic oscillators may still be used, provided that V_f as well as V_i may be approximated by a quadratic function in the Franck–Condon region. The value of ω_f chosen for the final state should be that for the best quadratic approximation to V_f in the Franck–Condon region, regardless of whether V_f is bound or unbound.

4. Polyatomic molecules

Several assumptions are required to apply this treatment to polyatomic molecules. Let the initial and final potential functions be given by, respectively,

$$V_i = \sum_{k=1}^{j} V'_k(q_k),$$

$$V_f = V_i + C + \sum_{k=1}^{j} \Delta V_k(q_k),$$

where q_k is one of a set of j normal coordinates referenced to the initial state equilibrium geometry. Let the wavefunctions be separable according to

$$\psi_f = \prod_{k=1}^{j} \psi''_k(q_k), \qquad \psi_i = \prod_{k=1}^{j} \psi'_k(q_k),$$

and the total energies be expressible (in dimensioned units) as

$$E_\mathrm{i} = T + V_\mathrm{i} = \sum_{k=1}^{L} (V_k' + T_k),$$

$$E_\mathrm{f} = T + V_\mathrm{f} = C + \sum_{k=1}^{L} (V_k' + \Delta V_k + T_k), \tag{3}$$

where T_k denotes the k-coordinate kinetic energy operator. It may be shown that the sum rules associated with the total overlap integral squared are

$$\langle (h\nu - C)^n \rangle = \left\langle \left(\sum_{k=1}^{L} \Delta V_k \right)^n \right\rangle, \quad n = 1, 2 \text{ only.} \tag{4}$$

The right hand side is decomposable into a sum of bracketed quantities which may be computed from eq. (1). For example, the mean and variance are given by

$$\langle h\nu \rangle = \sum_{k=1}^{L} \langle \Delta V_k \rangle + C,$$

$$\sigma^2 = \sum_{k=1}^{L} \sigma_k^2,$$

where

$$\sigma_k^2 = \langle (\Delta V_k)^2 \rangle - \langle \Delta V_k \rangle^2.$$

Thus, as with the diatomic case, the spectral width and mean frequency may be readily computed without overlap integral evaluation.

5. The reflection principle

The reflection principle expression for the overlap integral squared for a diatomic molecule is [3]

$$|\langle \psi_\mathrm{f} | \psi_\mathrm{i} \rangle|^2 \approx |\psi_\mathrm{i}(q)|^2 |\mathrm{d}V_\mathrm{f}/\mathrm{d}q|^{-1}, \tag{5}$$

where $h\nu$ and q are related by $h\nu = V_\mathrm{f}(q) - E_\mathrm{i}$. One way to assess the accuracy of this expression is to use it in computing the mean frequency and variance and compare the results with the exact solution, eq. (1). For example, let us consider the simple model in which V_f is linear, $V_\mathrm{f} = \delta^2/2 - q\delta$. Eq. (1) gives $\langle h\nu \rangle / \hbar\omega_\mathrm{i} = \delta^2/2 - (v' + \frac{1}{2})/2$ for the exact overlap integral, while the reflection principle predicts $\langle h\nu \rangle / \hbar\omega_\mathrm{i} = \delta^2/2 - (v' + \frac{1}{2})$. Clearly, the reflection principle errs substantially, especially in its prediction of the mean frequency at high v levels.

The source of these shortcomings of the reflection principle lies in its incorrect treatment of momentum. The physical interpretation behind eq. (5) is that the electronic "jump" occurs vertically at a particular internuclear distance q to the final state whose turning point is at q. The final state momentum at q is therefore zero, regardless of the initial state momentum. The reflection principle thus violates the conservation of momentum, a principle whose applicability to electronic spectra was stated by Mulliken [7] and has been confirmed by semiclassical calculations [8]. To conserve momentum one must require that the jump terminates instead at a state having energy E_f such that its kinetic energy, $E_\mathrm{f} - V_\mathrm{f}(q)$, equals the initial kinetic energy, $E_\mathrm{i} - V_\mathrm{i}(q)$. This modification leads to an alternative reflection principle expression,

$$|\langle \psi_\mathrm{f} | \psi_\mathrm{i} \rangle|^2 \approx |\psi_\mathrm{i}(q)|^2 |\mathrm{d}\Delta V/\mathrm{d}q|^{-1}, \tag{6}$$

where $h\nu = \Delta V(q)$. This modified reflection principle has the interesting property that, when used to compute mean values $\langle (h\nu)^n \rangle$ for continuous spectra, eq. (1) is satisfied for *all* n. That is, the modified reflection principle correctly predicts the mean frequency and width, but fails to correctly predict quantities $\langle (h\nu)^3 \rangle$, etc. For discrete spectra, eq. (1) is not strictly satisfied, since quantization of $h\nu$ restricts $\Delta V(q)$ to discrete values, although it is inherently a continuous variable.

6. Illustrations

Example A. Harmonic potentials: $\omega_\mathrm{i} = \omega_\mathrm{f}, v' = 0$.

The exact overlap integral squared for this model using the initial ground state wavefunction is the Poisson distribution function [9]

$$|\langle \psi_\mathrm{f} | \psi_\mathrm{i} \rangle|^2 = \mathrm{e}^{-\delta^2/2} \left(\frac{\delta^2}{2} \right)^{v''} \frac{1}{v''!}, \tag{7}$$

where v'' is the final state vibrational quantum number. The reflection principle solution (RP) is

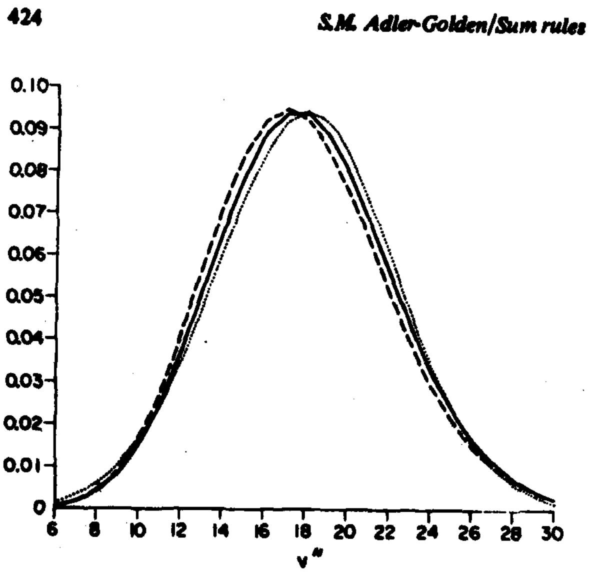

Fig. 2. Overlap integral squared versus final state vibrational quantum number for $\omega_f = \omega_i$, $\delta = 6$. —— = exact solution, ----- = RP approximation, ... = MRP approximation.

$$|\langle\psi_f|\psi_i\rangle|^2 \approx \frac{\exp\{-[\delta-(1+2v'')^{1/2}]^2\}}{[\pi(1+2v'')]^{1/2}}\,, \tag{8}$$

and the modified reflection principle solution (MRP) is the gaussian function

$$|\langle\psi_f|\psi_i\rangle|^2 \approx \frac{\exp[-(\delta/2-v''/\delta)^2]}{\delta\pi^{1/2}}\,. \tag{9}$$

In fig. 2 we display results for $\sigma = 6$. While as explained earlier the MRP yields a slightly more accurate value of the mean frequency than does the RP, both methods are comparable in terms of overall accuracy.

Example B. The Sulzer–Wieland equation

The Sulzer–Wieland equation [10,11] gives a simple relationship between the shape of the absorption spectrum of a diatomic molecule and its vibrational temperature. It states that the spectrum is gaussian, having σ^2 proportional to $\bar{E}_v$, the mean vibrational energy including zero point energy.

Although previously derived from the reflection principle using the linear V_f model discussed previously, a much more satisfactory derivation is obtained by instead applying the MRP to the harmonic oscillator model of example A. Indeed, for that model the proportionality of σ^2 to mean vibrational energy is rigorous: for a distribution of vibrational levels whose population in level v' is $P_{v'}$, we have, from eqs. (2a) and (2b),

$$\sigma^2 = \sum P_{v'}(\sigma_{v'})^2 = \sum P_{v'}(v'+\tfrac{1}{2})\delta^2(\hbar\omega)^2 = \delta^2\bar{E}_v\,. \tag{10}$$

This relationship clearly holds even for non-Boltzmann distributions.

Example C. Continuous spectra of halogens

As noted previously, the overall shape of a spectrum is largely unaffected by the behaviour of the potential functions outside of the Franck–Condon region, so that overlap integrals applicable to discrete spectra may also be used, with suitable modification, for bound-free spectra, or vice-versa. For example, the potentials in example A can be applied to a continuous spectrum, such as the visible spectrum of Br_2, by substituting the Stirling approximation for $n!$ into eq. (7) in order to extend its application to non-integer v''. (The Br_2 potentials strongly resemble those in example A in the Franck–Condon region.) The resulting expression is a good approximation to the correct overlap integral, as confirmed by the fact that the discrepancy between it and the RP expression [eq. (8)], ≲5%, is the same as that found between the exact and RP results in the Br_2 calculations [11].

Example D. Diffuse spectra of polyatomics: simple models

The Sulzer–Wieland result discussed in example B can be extended to many polyatomic molecules. It is frequently the case that $\omega_i \approx \omega_f$ for most of the normal modes of a molecule. With this assumption, results from the previous section yield

$$\langle h\nu\rangle = \text{constant and } \sigma^2 = \sum \delta_k^2 \bar{E}_k\,,$$

where $\bar{E}_k$ is the mean vibrational energy in the kth normal mode and δ_k is a constant for that mode. Furthermore, it has also been shown that the gaussian shape characteristic of diatomic absorption spectra often applies to polyatomic spectra as well, as in the case of alkyl halides [6]. Changes in the mean frequency with isotopic substitution [6] or with temperature are not accounted for by this simple model. These effects would arise, as in the diatomic case, if initial and final potential curvatures are not identical. In general, the shift in mean frequency will be given by a linear combination of $\bar{E}_k$'s.

A specific case in which eq. (11) is grossly inapplicable is when the final electronic state is dissociative along an asymmetric stretching coordinate, i.e., has a symmetrical "hump" rather than a well. R (defined previously) will be negative, hence, according to eq. (2a), $\langle h\nu \rangle$ will be strongly red-shifted with increased vibrational excitation. An example is the Hartley ultraviolet band of ozone, where the terminal potential is the dissociative $^1B_2$ state [12]. Vibrationally excited ozone indeed has an absorption spectrum that is red-shifted relative to unexcited ozone [4,13,14].

In treating a fluorescence spectrum, it must be noted that the initial states that contribute to the spectrum are not simply the available states, but consist of only those states which are optically pumped at that specific wavelength. As an example, we consider the LIF spectra of polycyclic aromatic hydrocarbons taken over a wide temperature range [15]. The spectrum of pyrene excited at 310 nm displays an enhanced width at high temperatures; from eq. (11) we may infer that both ground and excited vibrational states are being excited at this wavelength. On the other hand, the spectrum of fluoranthene excited at 325 nm displays very little temperature dependence, so it may be inferred that mainly ground vibrational states are excited.

7. Limitations

As mentioned previously, a constant transition moment has been assumed in the derivation of the above formulas. This approximation is quite good in many instances (e.g., bromine [11]), but may be unsatisfactory in others, particularly where the initial states are highly excited vibrational levels. A second approximation was invoked for polyatomic molecules, namely, that both initial and final potential functions be separable into terms $V_k(q_k)$, where vibrational motion in both initial and final states is describable using the same set of normal coordinates q_k. This approximation is satisfactory when the initial and final state equilibrium geometries are similar. When they are dissimilar, a new choice of coordinates can often be made to maximize the separability of both V_i and V_f. However, on some potential surfaces (a possible example is the dissociative $^1B_2$ state of ozone) there may be no good choice of coordinates, the vibrational motions being strongly coupled in every possible set of coordinates. In this case it would be inappropriate to use eq. (4) to compute $\langle h\nu \rangle$ and σ^2. Instead, eq. (1) may be used if ψ_i is understood as the total vibrational wavefunction, $\psi_i(q_1, q_2, \dots q_j)$, and ΔV as the total difference potential surface, $\Delta V(q_1, q_2, \dots q_j)$. In the light of the foregoing limitations, caution and discrimination is urged in applying the formulas presented here to real molecules.

Acknowledgement

This work was supported by the Air Force Geophysics Laboratory, Hanscom AFB, under Contract F19628-80-C-0028.

Appendix: Proof of eq. (1)

The proof for $n = 1$ is analogous to, but simpler than, the following proof for $n = 2$:

$$\langle \psi_i | (\Delta V)^2 | \psi_i \rangle = \langle \psi_i | (E_f - E_i)^2 | \psi_i \rangle$$

$$= \langle \psi_i | E_f^2 | \psi_i \rangle - \langle \psi_i | E_f E_i | \psi_i \rangle$$

$$- \langle \psi_i | E_i E_f | \psi_i \rangle + \langle \psi_i | E_i^2 | \psi_i \rangle ,$$

where E_i and E_f denote hamiltonian operators. Let us substitute $E_f = \Sigma_f | \psi_f \rangle E_f \langle \psi_f |$. For example, the first term of the above four is

$$\langle \psi_i | E_f^2 | \psi_i \rangle = \sum_f \langle \psi_i | E_f | \psi_f \rangle E_f \langle \psi_f | \psi_i \rangle$$

$$= \sum_f \langle \psi_i | \psi_f \rangle E_f^2 \langle \psi_f | \psi_i \rangle .$$

Define $S = \langle \psi_i | \psi_f \rangle$, $S^* = \langle \psi_f | \psi_i \rangle$, $|S|^2 = SS^*$; then the first term is $\Sigma_f |S|^2 E_f^2$. Similar operations on the remaining three terms yield

$$\langle\psi_i|(\Delta V)^2|\psi_i\rangle = \sum_f |S|^2(E_f^2 - 2E_iE_f + E_i^2)$$

$$= \sum_f |S|^2(E_f - E_i)^2 = \langle(h\nu)^2\rangle,$$

completing the proof. The failure of eq. (1) for $n = 3$ and higher is explained as follows. Consider, for example,

$$\langle\psi_i|(\Delta V)^3|\psi_i\rangle = \langle\psi_i|(E_f - E_i)^3|\psi_i\rangle,$$

which yields eight terms upon expansion. One of the terms is

$$\langle\psi_i|E_fE_iE_f|\psi_i\rangle = \sum_f SE_f\langle\psi_f|E_iE_f|\psi_i\rangle.$$

If eq. (1) were to be satisfied for $n = 3$, this term would have to equal $\Sigma_f|S|^2E_f^2E_i$. However, this can be true if and only if $E_iE_f = E_fE_i$, which holds only in the special case $\Delta V = E_f - E_i =$ constant. This line of reasoning thus restricts eq. (1) to values $n < 3$ for the general case.

References

[1] G. Herzberg, Spectra of diatomic molecules (Van Nostrand, Princeton, 1950).
[2] E.U. Condon, Phys. Rev. 32 (1928) 858.
[3] E.A. Gislason, J. Chem. Phys. 58 (1973) 3702.
[4] J.W. Simons, R.J. Paur, H.A. Webster III and E.J. Bair, J. Chem. Phys. 59 (1973) 1203.
[5] T. Kleindienst and E.J. Bair, Chem. Phys. Letters 49 (1977) 338.
[6] A.A. Gordus and R.B. Bernstein, J. Chem. Phys. 22 (1954) 790.
[7] R.S. Mulliken, J. Chem. Phys. 55 (1971) 309.
[8] S.M. Adler, Ph.D. Thesis, Cornell University (1979).
[9] E. Hutchisson, Phys. Rev. 36 (1930) 410.
[10] P. Sulzer and K. Wieland, Helv. Phys. Acta 25 (1952) 653.
[11] R.J. Leroy, R.G. McDonald, and G. Burns, J. Chem. Phys. 65 (1976) 1485.
[12] P.J. Hay and T.H. Dunning, J. Chem. Phys. 67 (1977) 2290.
[13] S.M. Adler-Golden and J.I. Steinfeld, to be published.
[14] L.C. McDade and W.D. McGrath, Chem. Phys. Letters 73 (1980) 413.
[15] D. Coe and J.I. Steinfeld, Chem. Phys. Letters 76 (1981) 485.

Ultraviolet continuum spectroscopy of vibrationally excited ozone

14.

S. M. Adler-Golden,[a] E. L. Schweitzer, and J. I. Steinfeld

Department of Chemistry, Massachusetts Institute of Technology, Cambridge, Massachusetts 02139

(Received 5 November 1981; accepted 16 November 1981)

A model is presented for the Hartley ultraviolet spectrum of vibrationally excited ozone based upon infrared–ultraviolet double resonance spectroscopy and previous temperature-dependent absorption measurements. The double-resonance transient arises from a 3500 cm^{-1} red shift of the absorption spectrum of ozone excited into the stretching vibrational states, with respect to the ground vibrational state. The double-resonance method is used to study relaxation kinetics of vibrationally excited ozone and to measure infrared energy deposition resulting from CO$_2$ laser pumping. The energy deposition is found to scale linearly with sample pressure and with infrared fluence, except for excitation on-resonance, which is strongly saturated. The UV spectral model is also used to calculate the wavelength and temperature dependence of the O(^1D) photodissociation quantum yield, which is an important component of stratospheric photochemistry.

I. INTRODUCTION

The ultraviolet absorption spectrum of ozone is among the most important features of that molecule, one of the key species in stratospheric photochemistry.[1] Despite extensive study, many questions remain concerning the Hartley continuum, a strong and nearly structureless absorption feature in the vicinity of 200–300 nm. Another poorly understood yet important subject concerns properties of vibrationally excited ozone, an abundant species formed in the O+O$_2$ [+*M*] recombination process.[2-4] The ultraviolet spectrum of vibrationally excited ozone is a potentially critical ingredient in stratospheric modeling.

In this article, we discuss recent experimental and theoretical work which sheds further light on the ultraviolet spectroscopy and kinetic properties of vibrationally excited ozone. The experimental technique utilized is infrared–ultraviolet double resonance spectroscopy, in which the asymmetric stretching mode (ν_3) is pumped by a pulsed CO$_2$ laser and the Hartley absorption band is probed by a continuous UV source. The apparatus has been described previously[5]; minor modifications are mentioned herein. Similar experiments have also been performed independently by McDade and McGrath.[6,7] The IRUVDR work, combined with absorption spectrum data and *ab initio* calculations, yields a self-consistent model for the Hartley band spectroscopy of vibrationally excited ozone. Application of this model enables us to determine rate constants for vibrational energy transfer, obtain information on the IR laser excitation process, and evaluate the hypothetical influence of vibrational excitation on stratospheric ozone photolysis in the ultraviolet region.

II. SPECTROSCOPIC MODEL

Portions of the potential energy surfaces for the electronic states involved in the Hartley ultraviolet transition have been obtained from *ab initio* computations[8]; thus, Franck–Condon intensity calculations on the Hartley band are possible in principle. Unfortunately, such spectral calculations have yet to be performed, one major difficulty being the strong coupling between the two stretching motions on the upper surface. Nevertheless, a qualitative understanding of the shape of the Hartley band and its dependence upon vibrational excitation may be readily obtained from simple arguments. Let us assume that the total vibrational wave function may be approximated as

$$\psi(q_1, q_2, q_3) = \psi_{\text{bend}}(q_2)\,\psi_{\text{stretch}}(q_1, q_3)\ , \tag{1}$$

and that the lower and upper potential functions satisfy

$$V_u(q_1, q_2, q_3) - V_l(q_1, q_2, q_3)$$
$$= \Delta V_{\text{bend}}(q_2) + \Delta V_{\text{stretch}}(q_1, q_3)\ , \tag{2}$$

where q_2 is the bending coordinate and q_1, q_3 are the symmetric and asymmetric stretching coordinates, respectively. The essence of these equations is that bending vibrational motion is assumed to be decoupled from the stretching motions. The mean transition energy of the spectrum $\langle h\nu\rangle$ is then given [see Eq. (4) of Ref. 9] by

$$\langle h\nu\rangle = \langle\psi_{\text{bend}}|\Delta V_{\text{bend}}|\psi_{\text{bend}}\rangle$$
$$+\langle\psi_{\text{stretch}}|\Delta V_{\text{stretch}}|\psi_{\text{stretch}}\rangle\ . \tag{3}$$

The shift in the spectrum upon vibrational excitation in the bending mode may thus be written as

$$\langle h\nu\rangle_{010} - \langle h\nu\rangle_{000} = \langle\psi^1_{\text{bend}}|\Delta V_{\text{bend}}|\psi^1_{\text{bend}}\rangle$$
$$-\langle\psi^0_{\text{bend}}|\Delta V_{\text{bend}}|\psi^0_{\text{bend}}\rangle\ , \tag{4}$$

where the superscript refers to the bending quantum number. This expression may be evaluated from Eq. (2a) of Ref. 9 using the vibrational frequencies derived from the *ab initio* calculations, yielding a result of -150 cm^{-1}. Thus, one may conclude that excitation into the bending mode will cause only a small red shift in the spectrum. The small magnitude of the shift results from both ground and excited electronic state bending frequencies being roughly similar. As it is also predicted from the *ab initio* calculations (and has been demonstrated experimentally[10]) that the equilibrium

---

[a] Present address: Spectral Sciences Inc., Burlington, Mass. 01803.

The U.S. Government is authorized to reproduce and sell this report. Permission for further reproduction by others must be obtained from the copyright owner.

0021-9606/82/052201-09$02.10

© 1982 American Institute of Physics

bond angles are also quite similar in the two states, only a slight change in spectral breadth with bending excitation is expected. Thus, both (010) and (000) states of ozone should have Hartley absorption spectra of very similar shapes.

On the other hand, excitation into either of the stretching modes is predicted to have a very large effect upon the Hartley band. The upper potential has a double minimum along the q_3 direction,[8] hence excitation into the (001) state should yield a substantial red shift.[9] Also, at large displacements from the electronic ground state geometry, the upper surface should have a dissociative trench along the directions corresponding to the stretching of each bond separately; these directions are admixtures of both q_1 and q_3 coordinates. Thus, one expects that at the long-wavelength end of the spectrum, which reflects Franck–Condon overlap in the trench region, both (100) and (001) states may have comparably large absorption coefficients.

A spectral model for the Hartley band is suggested by the above discussion and may be summarized as follows. Denoting P_{ijk} as the fractional population of ground electronic state ozone in the (ijk) vibrational state, having an absorption coefficient $\epsilon_{ijk}(\nu)$, then at low excitations

$$\epsilon = P_{000}\epsilon_{000} + P_{010}\epsilon_{010} + P_{100}\epsilon_{100} + P_{001}\epsilon_{001} , \qquad (5)$$

where from the above arguments $\epsilon_{000} \approx \epsilon_{010}$. Furthermore, under conditions where P_{100} and P_{001} are in equilibrium, their populations are in roughly the same relative proportion, at and above room temperature. Therefore, we may write

$$P_{100}\epsilon_{100} + P_{001}\epsilon_{001} \approx (P_{100} + P_{001})\epsilon^* , \qquad (6)$$

where ϵ^* is the population-weighted average extinction coefficient for the first excited stretching modes. The final result is

$$\epsilon = (P_{000} + P_{010})\epsilon_{000} + (P_{100} + P_{001})\epsilon^* , \qquad (7)$$

which is a two-parameter approximation to the vibrationally excited Hartley continuum.

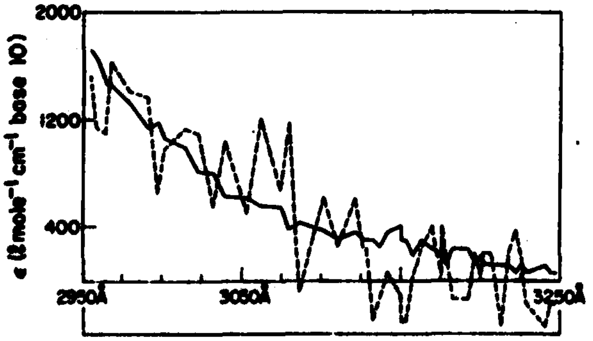

FIG. 1. The absorption spectrum of (100) plus (001) excited ozone ϵ^* in the 2950–3250 Å region. Dashed curve is the solution of three simultaneous equations based on Eq. (8), using spectra of 200, 300, and 333 K from Ref. 11. Solid curve is obtained by setting $\epsilon_{000} = \epsilon_{010}$ and using only the 200 and 333 K spectra.

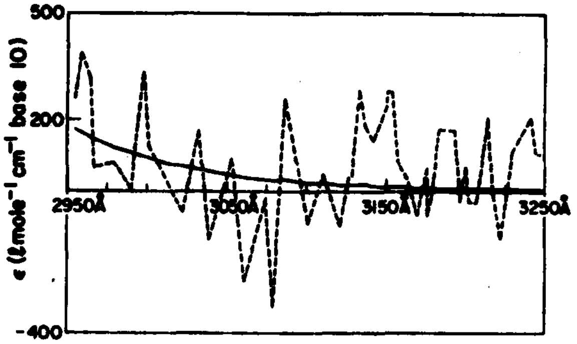

FIG. 2. Absorption spectra of ozone in the 2950–3250 Å region, obtained by solution of three simultaneous equations based on Eq. (8). Solid curve is ϵ_{000}, dashed curve is ϵ_{010}.

The spectral model expressed by Eq. (7) is subject to experimental verification. Several independent tests which lend support to this model are described below.

A. Temperature dependence

The most comprehensive study of the temperature-dependence of the Hartley band is the work of Simons *et al.*,[11] who measured spectra at 200, 300, and 333 K. Bair has provided us with the absorption coefficient data in tabular form, which is used in the following calculations. From Eqs. (5) and (6) we can obtain a three-parameter equation

$$\epsilon = P_{000}\epsilon_{000} + P_{010}\epsilon_{010} + (P_{100} + P_{001})\epsilon^* , \qquad (8)$$

from which it is possible to solve explicitly for ϵ_{000}, ϵ_{010}, and ϵ^* given the three experimental spectra. In practice, the solutions are very sensitive to experimental errors, such as normalization of the spectra, due to the weakness of the temperature dependence. For this reason, we have restricted the analysis to the spectral region where the temperature effect is greatest. The solutions of Eq. (8) are depicted in Figs. 1 and 2. The "noise" arises from the small amount of structure present in the original spectra. It is observed that, to within the noise level, the hypothesis that $\epsilon_{000} \approx \epsilon_{010}$ is confirmed. The conjecture by Bair and others[11,12] that ϵ_{010} is red shifted by ~700 cm⁻¹ relative to ϵ_{000} appears to be unjustified.

B. IRUVDR experiments

In the infrared–ultraviolet double resonance experiments,[5–7] the CO_2 laser populates the (001) state, which rapidly equilibrates with the (100) state; then both levels decay according to the same double exponential function as is observed in infrared fluorescence experiments.[13,14] Equation (7) implies that the absorbance transient observed following laser excitation should be proportional to the excited stretching mode population and, thus, should obey the same time dependence. This behavior has previously been demonstrated in the 254 nm region,[5] and new measurements using interference filters at 289 and 313 nm also yield the same results. The rate constants for vibrational energy transfer measured

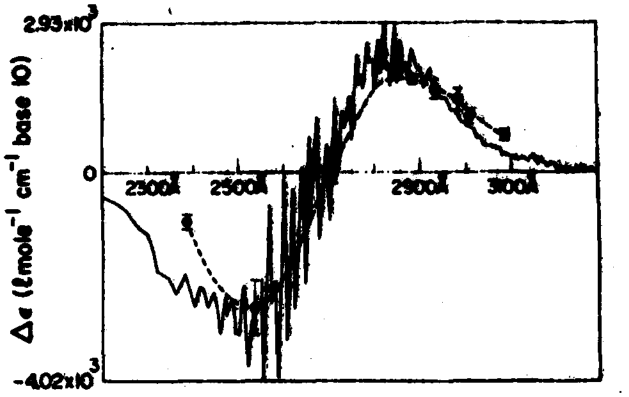

FIG. 3. Dependence of the magnitude of the IRUVDR transient upon wavelength. Solid curve is $\epsilon^* - \epsilon_{000}$, from the 200 and 333 K data of Ref. 11. The dashed curve connects the IRUVDR data points, the vertical scaling having been adjusted so that the amplitudes of the two curves are similar.

at all three wavelengths agree well with results obtained via infrared fluorescence,[13,14] as has been discussed previously.[5]

Another test of the assumption that $\epsilon_{010} = \epsilon_{000}$ can be derived from the wavelength dependence of the IRUVDR transients. According to Eq. (7) the change in the spectrum with temperature, being due solely to ozone excited in the stretching modes, should scale with the laser-induced transients. By adding a monochromator to the previously described apparatus,[5] we measured the magnitude of the initial transient at a number of wavelengths relative to that at 280 nm. We found that by using an appropriate scaling factor, the laser-induced transients could indeed approximate the temperature-induced absorbance change rather well, as is shown in Fig. 3. The slight red shift of the spectrum derived from IRUVDR relative to that derived from the temperature dependence may be due to a small quantity of multiply excited vibrational levels.

Several other IRUVDR measurements are capable of testing the spectral model developed here. One measurement involves choosing $\lambda = 271$ nm, where the instantaneous laser transient is found to be zero,[7] hence $\epsilon_{000} = \epsilon^*$. If ϵ_{010} were significantly different from ϵ_{000} at that wavelength, then a transient corresponding to (010) population would appear. However, none is observed, either in the current or in previous work.[7] A small, gradual, downward shift of the absorbance does occur on a relatively long time scale. We ascribe this to rarefaction of the sample caused by the temperature rise accompanying the $V \rightarrow T$ process.

Equation (7) may also be tested by an analysis of IRUVDR signals which possess a slow decay component, such as those at 3100 Å displayed in Refs. 6 and 7. This component has been assigned to thermally equilibrated ozone,[6] and its magnitude is therefore related to the quantity of vibrationally excited ozone initially formed. For the data of Refs. 6 and 7, Eq. (7) predicts a fractional excitation $[O_3^{\ddagger}]/[O_3]_{\rm total}$ of 0.115 ± 0.020 based on the magnitude of the initial transient, and assuming a value for $\epsilon^*/\epsilon_{000} = 12 \pm 2$. In that range of excitation, the quantity of (100) plus (001) vibrationally excited ozone remaining after thermal equilibration is 0.10 of that initially produced by the laser pulse (in pure ozone), hence Eq. (7) predicts that the magnitude of the slow decay component should be 0.10 of that of the initial transient. Experimentally, the amplitude of the slow decay component is found to be 0.11 ± 0.03 of that of the initial transient, in excellent agreement with the preceding estimate. A potential complication would be the partial transparency induced by sample rarefaction, as discussed above, but at 310 nm this should affect the slow component by only about 10% of its magnitude, and can therefore be neglected. Thus, it is seen that Eq. (7) satisfactorily describes the absorbance at 310 nm over the range $0.01 \lesssim [O_3^{\ddagger}]/[O_3]_{\rm total} \lesssim 0.1$.

A major difficulty in the determination of ϵ^* by the IRUVDR method is in measuring accurately the quantity of vibrationally excited ozone to which the UV absorbance transient corresponds. In principle, this can be done by observing attenuation of the infrared beam passing through the sample. This proved to be a difficult measurement under our normal experimental conditions, however. A beam attenuation measurement under conditions of high excitation is described below, in Sec. III B 1.

C. Comparison of absorption spectra of vibrationally excited ozone

According to Eq. (7), it is sufficient to determine $\epsilon^*(\nu)$ in order to explain satisfactorily the spectrum of ozone excited to low levels of excitation. There are two ways to obtain ϵ^*, the most direct being from the IRUVDR transients. The main difficulty is in the measurement of the quantity of vibrationally excited ozone formed in the laser pulse, as noted above. In the previous section we have estimated the fractional excitation for the experimental conditions of Refs. 6 and 7, viz. (0.115 ± 0.020), which fortuitously coincides with the value which was used therein in the determination of ϵ^*. The spectrum shows a broad peak at 2850 Å and falls off somewhat more sharply to the blue than to the red, reaching a near zero value at around 2500 Å.[7]

Another way to obtain ϵ^* is from the difference between spectra taken at different temperatures. Figure 4 depicts ϵ^* determined from the 333 and 200 K spectra of Simons *et al.*[11] Due to the weakness of the temperature dependence the spectrum is not highly accurate, especially away from the red end. A possible error in relative normalization of the original spectra would be especially troublesome, and a residue of structure in those spectra gives ϵ^* an artificially jagged appearance. Despite these deficiencies the spectrum is strikingly similar to the IRUVDR result of Ref. 7. The ϵ^* spectrum also bears a strong resemblance to the "ozone precursor" spectrum observed by several others during formation of ozone from oxygen at atmospheric pressure,[15,16] and which has been ascribed to vibrationally excited ozone.[16,17]

In summary, the approximate shape of the ϵ^* spec-

17.

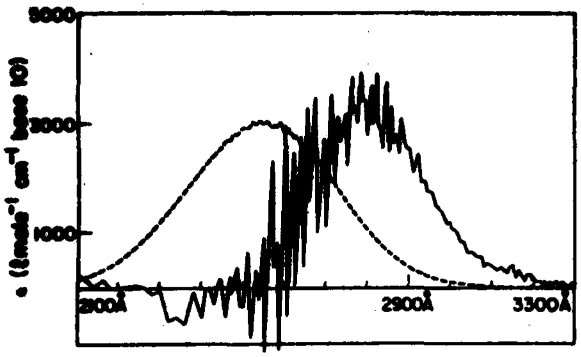

FIG. 4. The Hartley absorption spectrum of ozone. The dashed curve is the 200 K spectrum, and the solid curve is the vibrationally excited spectrum ϵ^*, a portion of which is displayed in Fig. 1.

trum has been determined from both the temperature dependence of the UV absorption spectrum and the IRUVDR measurements in Ref. 7. While more accurate data on the Hartley absorption continuum are clearly needed, the existing data are useful for a number of applications. Several such applications are discussed in the following section.

III. APPLICATIONS OF THE SPECTRAL MODEL

A. Rate constants for vibrational energy transfer

The alteration of the Hartley continuum caused by vibrational excitation finds a very useful application in the determination of rate constants for vibrational energy transfer by IRUVDR. Its extremely high sensitivity and the absence of systematic error may make it the method of choice for the study of relaxation rates for the singly excited vibrational levels of ozone, as has been discussed previously.[5] In Ref. 5, we estimated a crude lower limit for the rate of the rapid $\nu_3 \rightleftharpoons \nu_1$ equilibration process, on the order of 10^6 Torr^{-1} s^{-1}, from the "induction time" of the initial IRUVDR transient. These measurements have now been repeated at much lower ozone pressures, using an improved apparatus, employing collinear infrared and ultraviolet beams in either a 120 or a 20 cm cell, similar to the configuration of Ref. 6. Using an interference filter at 289 nm, the wavelength of greatest sensitivity, we were able to achieve a detection limit of about 10^{12} molecules cm^{-3} of $O_3^\dagger$, by averaging over several hundred laser pulses. At a total pressure of 0.07 Torr the transient was observed to be essentially instantaneous to within the combined response time of the electronics and laser pulse width, around 1 or 2 μs. Thus, the previously reported induction time should be attributed to electronic interference from the laser, rather than to any kinetic process.

There are two possible explanations for the virtually instantaneous onset of the transient. One is that the $(001) \rightleftharpoons (100)$ equilibration occurs within the observed rise time, requiring a nearly gas kinetic collision rate. Since the energy transfer per collision is only 60 cm^{-1}, this explanation is certainly plausible. A second possible explanation is that $\epsilon_{100} \approx \epsilon_{001}$ at 289 nm, making the equilibration process incapable of observation. To distinguish between these hypotheses one should take measurements of comparable sensitivity over a range of wavelengths, it being unlikely that $\epsilon_{100} \approx \epsilon_{001}$ for all wavelengths. We have carried out some measurements in the 294 and 310 nm regions which yielded similar results as at 289 nm; however, due to lower sensitivity the ozone pressures required were several times greater. Thus, it is not possible to establish unambiguously a value for the $(001) \rightleftharpoons (100)$ equilibrium time from this experiment.

B. Vibrational energy deposition following CO_2 laser irradiation

The excitation of molecular species by high-intensity infrared radiation is a widely studied but still incompletely understood process.[18] At very high laser intensities, ozone is reported to undergo multiple-photon dissociation[19]; at lower intensities, such as those available from an unfocused CO_2 laser beam, the excitation process is surely less complex, but by the same token, the low-intensity excitation regime may be more readily understood, especially given the well-known spectroscopy of the low vibrational levels. The IRUVDR method provides a convenient and sensitive technique for measuring the fractional excitation of ozone $[O_3^\dagger]/[O_3]_{\text{total}}$. We denote this quantity by $\langle n \rangle$, the mean number of IR photons absorbed by molecule, since at the low levels of excitation studied here the population of multiply excited ozone molecules is negligibly small. We present experimental results for $\langle n \rangle$ as a function of total pressure $(O_3 + O_2)$, and infrared frequency and fluence in the single-photon regime, along with model calculations which aid in interpreting the data.

1. *Experimental measurements*

Most of the data were obtained from measurement of the UV transient using a 289 nm interference filter. Collinear infrared and ultraviolet beams were employed in a $l = 20$ cm cell, care being taken to insure complete overlap of the UV beam by the IR beam. The sensitivity was sufficient to allow single-shot measurements of the transient. Infrared fluence passing through the rear iris with the cell evacuated was measured with a Scientech 380102 power meter. The fluence measurements represent an average over the beam area, the actual beam intensity displaying interference fringes resulting from passage through the irises and a germanium beam splitter. The ~20 nm bandwidth of the UV filter posed a potential problem due to wavelength variation of absorption coefficients of O_3 and $O_3^\dagger$. Fortunately, however, the 289 nm wavelength lies near a flat portion of the $\Delta\epsilon = \epsilon^* - \epsilon_{000}$ curve (see Fig. 3). A reasonably well-determined value of $\Delta\epsilon = 2.6 \times 10^3$ ℓ mol^{-1} cm^{-1} (base 10) may be therefore assigned on the basis of the spectral model in order to relate the transient absorbance ΔA to the quantity of $O_3^\dagger$ produced, via the equation $\Delta A = [O_3^\dagger] l \Delta\epsilon$.

Despite the wealth of evidence presented earlier to support the basic validity of the spectral model, its

18.

absolute accuracy has not yet been quantified. Hence, the value of $\Delta\epsilon$ cited above, and thus the corresponding value of $\langle n \rangle$, are of unknown accuracy. We therefore carried out a double check on the above method for determining $\langle n \rangle$ by using a sufficiently high pressure of O_3 and total pressure (~3 Torr O_3 in 10 Torr total pressure) to obtain measurable attenuation of the CO_2 laser beam during passage through the cell, thus establishing a direct determination of deposited infrared energy. Unfortunately, the UV optical density at that ozone pressure is too great to permit a simultaneous measurement of the 289 nm transient. We circumvented that problem by using a 313 nm interference filter instead, and scaling the ΔA value measured at 313 nm to a hypothetical value at 289 nm, using the previously measured ratio between the IRUVDR transients at these two wavelengths. The resulting value of $\langle n \rangle$ was about 40% lower than that determined directly by infrared transmission in two separate experiments. Considering the uncertainties in the measurements and in the value of $\Delta\epsilon$, and in view of the possible influence of multiply excited vibrational levels ($\langle n \rangle$ was about 0.2 in these measurements), this agreement is tolerable.

We conclude that the technique of determining $\langle n \rangle$ from IRUVDR transients may be subject to a systematic error of up to 40%. However, as it is likely that much of this discrepancy is related to the conditions employed in this particular experiment, the data which follow, taken at lower degrees of excitation and using the 289 nm bandpass filter, are probably of considerably better accuracy. The precision of an individual measurement, arising principally from variations in infrared laser fluence passing through the cell, is on the order of ±20%.

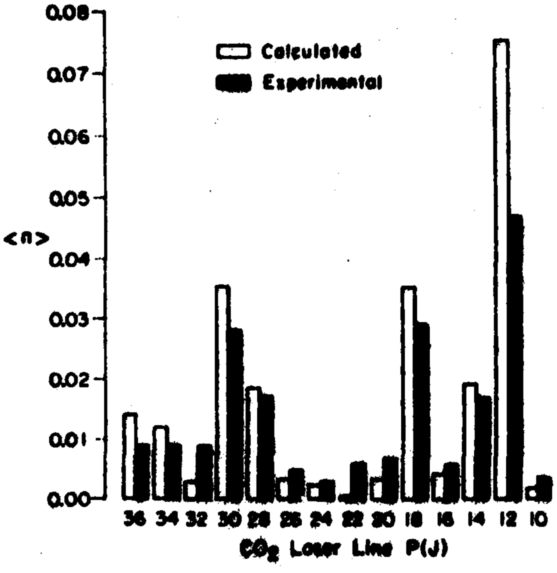

FIG. 5. Mean fractional excitation of ozone by CO_2 laser irradiation for different laser lines in the 9.6 μm *P* branch. Solid bars denote experimental data, open bars denote model calculations (see the text). Ozone pressure is 0.6 Torr, oxygen pressure is 2.4 Torr. The experimental laser fluence is 0.04–0.06 J/cm^2 for these lines, 0.05 J/cm^2 being used in the model calculations.

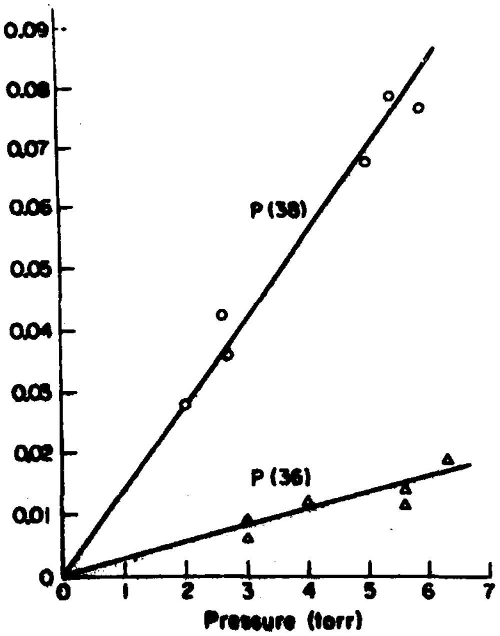

FIG. 6. Experimental dependence of $\langle n \rangle$ upon total pressure, for CO_2 *P*(36) and *P*(38) lines, at a fluence of 0.034 J/cm^2, and a composition of 10% ozone in oxygen.

Typical experimental results for $\langle n \rangle$ are depicted in Figs. 5 through 7. Pumping of ozone was observed using *all* of the available CO_2 laser lines in the 9.6 μm *P* branch, the strongest pumping occurring with lines, such as *P*(12) and *P*(30), that are resonant with O_3 absorption lines (see Fig. 5). With a sampling of both on- and off-resonant laser lines, we found $\langle n \rangle$ to be linearly proportional to total pressure (at a fixed ozone mole fraction) to within experimental error in the 2 to 6 Torr range studied (see Fig. 6). The dependence of $\langle n \rangle$ upon laser fluence was studied by attenuating the laser beam with polyethylene sheets. With several off-resonant lines, the signal was found to be linearly proportional to fluence, but with on-resonant lines the amplitude of the IRUVDR transient showed marked saturation behavior, as is shown in Fig. 7.

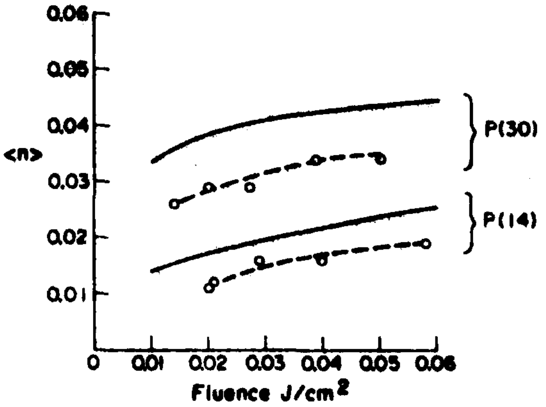

FIG. 7. Dependence of $\langle n \rangle$ upon laser fluence for on-resonance CO_2 laser lines. Solid curves denote model calculations (see the text).

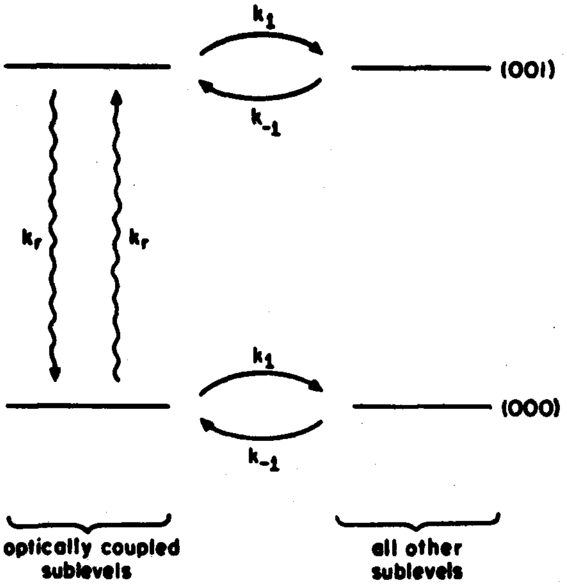

FIG. 8. Kinetic model for vibrational excitation of ozone in the laser field.

The dependence of $\langle n\rangle$ upon mole fraction of ozone was not explored, dilute mixtures of ozone in oxygen being used in most measurements. However, some observations were made using the CO_2 $P(30)$ line and the apparatus described in Ref. 5, which demonstrated decreasing values of $\langle n\rangle$ with increasing ozone concentration, especially at high values of $\langle n\rangle$. This may be due to attenuation of the laser beam upon transmission through the sample. As the ozone absorption lines are quite narrow, they may be capable of selectively absorbing the most closely resonant frequency components of the CO_2 laser output, thus "burning a hole" in the laser's output spectrum. This point is discussed more fully in the following section.

2. *Excitation model*

In order to gain insight into the experimental results, we have carried out some model calculations for $\langle n\rangle$. The kinetic scheme utilized is depicted in Fig. 8. In brief, the upper and lower rotational sublevels associated with an ozone absorption line near the laser frequency are optically coupled to each other in the presence of the laser field by the radiative rate constant k_r, and are assumed to be collisionally coupled to the remaining rotational sublevels in each vibrational state by the pseudo-first-order rate constants k_1 and k_{-1}. This "four-box" model has been previously employed by us to describe the kinetics of infrared saturation,[20] passive *Q* switching,[21] and infrared double-resonance experiments employing CO_2 lasers[22] and tunable diode lasers.[23] In the pressure range of interest here, vibrational deactivation during the ~1 μs laser pulse may be neglected.

While the model depicted in Fig. 8 may be solved exactly,[23] a much less cumbersome and sufficiently accurate solution is the following expression, derived by assuming steady-state concentration in the optically coupled sublevels

$$\frac{d\langle n\rangle}{dt}=\frac{\beta k_1/2}{1+k_1/2k_r}\,, \tag{9}$$

where $\beta=k_{-1}/(k_1+k_{-1})$, the equilibrium population in the pumped rotational sublevel. Integrating over the laser pulse duration and summing over all ozone absorption lines which appreciably interact with the laser radiation yields the net $\langle n\rangle$ value. (In practice, only lines within about 0.1 cm^{-1} of the laser frequency need to be included for the maximum fluence considered here, approximately 0.05 J/cm^2.) The radiative rate constant k_r can be written as[24]

$$k_r=I\sigma(\bar{\nu})/h\nu\beta \tag{10}$$

for monochromatic radiation. In the present situation, Eq. (10) must be modified to take account of the distribution of frequencies in the laser output arising from the longitudinal mode structure. This can be done by integrating Eq. (10) over a normalized intensity distribution function $I(\bar{\nu})$, to be specified a little later, giving

$$k_r=\int I(\bar{\nu})\,\sigma(\bar{\nu})\,d\bar{\nu}/h\nu\beta\,, \tag{11}$$

where $\bar{\nu}$ denotes wave number in cm^{-1}, $I(\bar{\nu})$ is the radiation intensity in W per cm^2 per cm^{-1}, and $\sigma(\bar{\nu})$ is the photon absorption cross section in cm^2 per cm^{-1}. The cross section $\sigma(\bar{\nu})$ may be approximated by the homogeneous line shape function

$$\sigma(\bar{\nu})=\frac{S}{\pi}\left[\frac{\delta\bar{\nu}}{(\bar{\nu}-\bar{\nu}_0)^2+(\delta\bar{\nu})^2}\right]\,, \tag{12}$$

where S is the integrated line strength in cm^2, $\bar{\nu}_0$ the resonant wave number, and $\delta\bar{\nu}$ is the half-width at half-height of the absorption line. We assume that inhomogeneous broadening may be neglected.

The usual Lorentzian power-broadened line shape expression for absorbed energy versus detuning[24,25] may be obtained by combining Eqs. (9), (10), and (12). The use of Eq. (11) instead of Eq. (10) simply gives a broader function. No attempt is made to include the effect of laser beam attenuation; thus, this treatment is applicable only to optically thin samples.

It remains to find appropriate input parameters for the above equations. The linewidth $\delta\bar{\nu}$ is taken as the collision-broadened half-width, found to be 0.08 $cm^{-1}\,atm^{-1}$ for O_3–O_2 collisions and 0.15 $cm^{-1}\,atm^{-1}$ for O_3–O_3 collisions.[26] The ozone line positions are taken from Ref. 27, and the integrated line intensities are from the same reference, but multiplied by 1.113, in accordance with more recent work.[28] The population relaxation rate constant k_1 was set equal to the dephasing rate constant $k_2=2\pi c\delta\bar{\nu}$ in accordance with observations on similar molecules.[29] The temporal shape of the laser pulse is an important input variable; we determined this experimentally with a photon–drag detector. It is a typical "TEA-laser" pulse profile, with an initial spike of 40–50 ns duration containing ~60% of the total pulse energy, and a low-intensity tail, lasting a little less than 1 μs, containing 40% of the pulse energy. For

20.

modeling purposes, this was approximated as a flat-topped pulse function by a flat line lasting for twice the spike duration, with the intensities adjusted to give the proper fluence ratios. Best results were obtained with a total pulse duration of 0.5 μs, which is somewhat shorter than the observed pulse length. The use of the shorter total duration may be rationalized in either of two ways. First, it may be correct for the presence of oscillatory mode structure present in the actual pulse shape, which may compress the effective time during which the laser is on. An alternative rationale is that decreasing the effective pulse duration may instead be a means of compensating for a discrepancy between k_1 and k_2; halving the pulse duration is, in fact, equivalent to using a k_1/k_2 ratio of 0.5.

The remaining parameter which required trial-and-error fitting concerned the laser intensity distribution function $I(\nu)$; the choice of this parameter particularly influenced the degree of off-resonance pumping. The laser line shape is expected *a priori* to consist of narrow cavity modes with a spacing of 0.[illegible] cm^{-1}, whose intensity envelope thus follows the [illegible] line shape (0.06 cm^{-1} FWHM for the laser gas mixture used), which is truncated at the zero-gain threshold. Since the precise locations of the [illegible] and most likely vary during the course of the experiment, we felt it best to [illegible] a [illegible] line shape having the [illegible]. The triangular line shape [illegible] an analytical solution to Eq. (11) [illegible] values of ⟨ν⟩ found for [illegible] very sensitive to the [illegible] the [illegible]. The calculations presented in [illegible] a laser full width of 0.0[illegible] cm^{-1}.

The [illegible] values of ⟨ν⟩ [illegible] (see Fig. 5) [illegible] in Fig. 7.

In summary, the degree of vibrational excitation of [illegible] may be pre[illegible] a wide range of [illegible] by using model

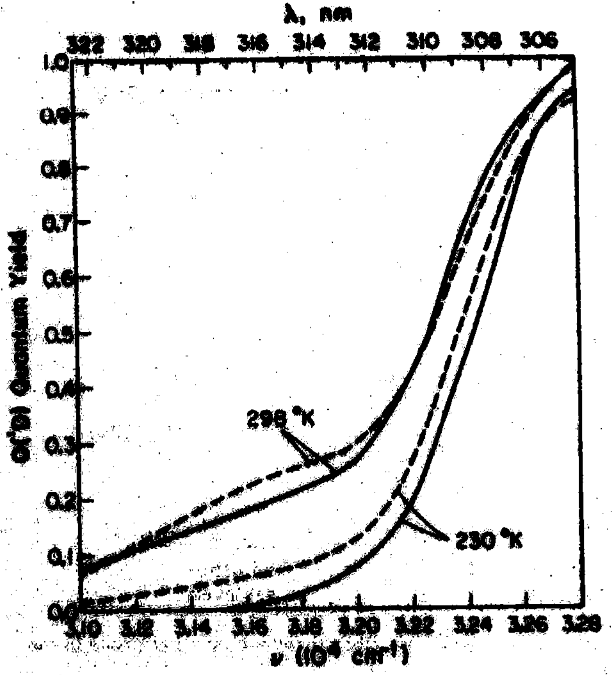

FIG. 6. O(^1D) quantum yields vs photolysis wavelength. Solid lines are experimental determinations (Refs. 34 and 35) and dashed lines are from the model calculations described in the text. [illegible] data (Ref. 34) have been renormalized to unity at [illegible] nm.

calculations to extend the range of experimental data. With [illegible] parameters, [illegible] regarding the [illegible] of the [illegible], and by in[illegible] through the [illegible], [illegible] and calculation [illegible].

C. O(^1D) production in the near ultraviolet photolysis of ozone

The photolysis of ozone in the Huggins–Hartley ultraviolet region yields both O(^1D) and O(^3P) atoms; in the [illegible], the O(^1D) atoms thus formed are the major source of [illegible]. Much interest has, therefore, [illegible] the quantum yield for O(^1D) production from [illegible], especially in the "fall off region" of [illegible] where considerable ultraviolet flux penetrates the lower atmosphere.[illegible] In this fall off region it is found that the O(^1D) quantum yield declines rapidly from a value close to unity at 300 nm towards a negligibly small value near 325 nm, the precise position and steepness of the decline being strongly temperature dependent[34-36] (see Fig. 6). The ability to model these data is important, not only in terms of parametrizing the quantum yield function for a wide range of wavelengths and temperatures, but also in providing an understanding of the photolysis mechanism.

Previous attempts at modeling the fall off region data have focused primarily on the role of rotational energy in contributing to the total energy required to reach the O(^1D) production threshold. However, retational energy alone does not explain the observed temperature dependence.[33] Recent investigations have suggested that vibrational excitation is also important in the photolysis process. Zittel and Little[37] have observed a greatly enhanced O(^1D) production cross section in the red end of the Hartley band following IR laser excitation. They ascribe this effect to vibrationally excited ozone having a large absorption cross section in that spectral region. The temperature dependence of the absorption coefficient, as seen, e.g., in the data of Ref. 11, is consistent with that premise. Hudson[38] has utilized those absorption data in quantum yield model calculations which give good agreement with experiment. A drawback of those calculations is that, unfortunately, the absorption data alone are not sufficient to specify uniquely a spectroscopic model for the ozone ultraviolet spectrum.

In this paper, we have presented a model for the Hartley absorption spectrum of vibrationally excited ozone, based on Eq. (7), which is well-supported by the IRUVDR experiments, and thus can provide a reasonable starting point for O(^1D) quantum yield modeling. Extension of Eq. (7) into the longer wavelength Huggins region poses no conceptual problem, even if, as has been proposed,[39] the Huggins bands belong to another electronic transition. This is because we can reasonably assume that, in the fall off region, the major contribution to the vibrationally excited spectrum is the tail of the (100) plus (001) excited ozone spectrum depicted in Fig. 4, and belonging to the Hartley transition. Even further to the red, where the "hot" Huggins spectrum appears to be discrete, it is still found that transitions originating from (100)- and (001)-excited ozone possess greater intensity than those originating from (010),[40] and thus dominate the spectrum of vibrationally excited ozone.

Proceeding with the calculation according to the method of Moortgat *et al.*[33] we assume that the total internal energy (vibrational plus rotational) adds fully to the energy acquired from the ultraviolet photon, and that for a given total energy the O(^1D) quantum yield varies as a ramp function from zero at a selected threshold energy to unity at a higher energy, taken here to be 600 cm^{-1} above the threshold. The classical density of rotational states $\propto (E_{rot})^{1/2}$ is fully satisfactory for this

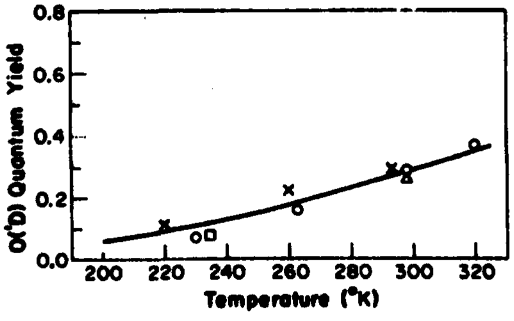

FIG. 10. O(^1D) quantum yields at 313 nm vs temperature. ○ = Ref. 33 data, △ = Ref. 34, □ = Ref. 35, × = Ref. 36; solid line is the model calculation described in the text.

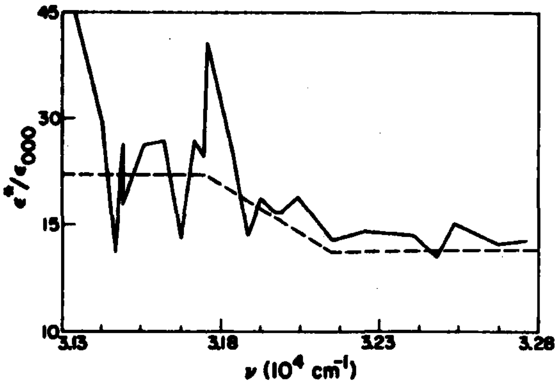

FIG. 11. The ratio $\epsilon^*/\epsilon_{000}$ in the 31 300–32 800 cm^{-1} region (solid curve). For purposes of modeling the O(^1D) photodissociation quantum yield, as described in the text, the smooth dashed curve is used instead.

calculation. The quantum yield for the ground, first excited stretching and first excited bending levels are computed separately, weighted according to their absorption coefficient and population, and combined to give the net O(^1D) quantum yield $\overline{Q}$ as follows:

$$\overline{Q} = \frac{\Sigma \epsilon_{ijk} P_{ijk} Q_{ijk}}{\Sigma \epsilon_{ijk} P_{ijk}} , \tag{13}$$

where ϵ_{ijk}, P_{ijk}, and Q_{ijk} are the absorption coefficient, population and O(^1D) quantum yield, respectively, of the (ijk) vibrational level. According to Eq. (7), this reduces to

$$\overline{Q} = \frac{\epsilon_{000}(P_{000} Q_{000} + P_{010} Q_{010}) + \epsilon^* P^* Q^*}{\epsilon_{000}(1 - P^*) + \epsilon^* P^*} , \tag{14}$$

where $P^* = P_{100} + P_{001}$. The above equation requires knowledge of ϵ^* / ϵ_0 in the fall off region, which is taken to be the ramp function depicted in Fig. 11. The O(^1D) threshold energy was adjusted for best fit between calculations and experiments, yielding a value of (32 900 ± 100) cm^{-1}.

The comparison of experimental and calculated results appears in Figs. 9 and 10. Good agreement is seen in the wavelength dependence of the quantum yield over the 305–322 nm range at both low and room temperatures. At 313 nm, the agreement between the calculation and a large number of experimental results is excellent over the full temperature range studied. It should be noted, however, that the long wavelength tail above 313 nm, appearing in the Brock and Watson[34] data depicted in Fig. 9 and predicted as well by this calculation, conflicts with the majority of experimental studies, which instead show a more rapid decline of the quantum yield. Until this issue is resolved the validity of the model calculation remains open to question. Its success at and below 313 nm does, however, suggest that vibrationally excited ozone does indeed play an important role in stratospheric ozone photolysis.

IV. CONCLUSIONS

A model for the Hartley ultraviolet spectrum of vibrationally excited ozone has been presented and applied to

22.

problems involving vibrational energy transfer, infrared energy deposition resulting from pumping by a CO_2 laser, and stratospheric ozone photodissociation. In the latter instances, simple models have been presented which are capable of reproducing the experimental results quite well. Many other molecules possess strong, continuous ultraviolet absorption spectra, as well as infrared resonances near CO_2 laser lines; the alkyl halides are just one example.[41] Many of these species may therefore be excellent candidates for study by the methods described here.

ACKNOWLEDGMENTS

This work was supported by the Air Force Geophysics Laboratory under Contract No. F19628-80-C-0028. We would like to thank Dr. R. Pack, Dr. R. Hudson, and Dr. E. Bair for helpful discussions.

[1] H. Okabe, *Photochemistry of Small Molecules* (Wiley, New York, 1978).

[2] C. W. von Rosenberg, Jr., and D. W. Trainor, J. Chem. Phys. 61, 2442 (1975).

[3] C. W. von Rosenberg, Jr., and D. W. Trainor, J. Chem. Phys. 63, 5348 (1975).

[4] W. T. Rawlins, G. E. Caledonia, and J. P. Kennealy, J. Geophys. Res. 86, 5247 (1981).

[5] S. M. Adler-Golden and J. I. Steinfeld, Chem. Phys. Lett. 76, 479 (1980).

[6] I. C. McDade and W. D. McGrath, Chem. Phys. Lett. 73, 432 (1980).

[7] I. C. McDade and W. D. McGrath, Chem. Phys. Lett. 73, 413 (1980).

[8] P. J. Hay and T. H. Dunning, J. Chem. Phys. 67, 2290 (1977).

[9] S. M. Adler-Golden, Chem. Phys. (in press).

[10] R. K. Sparks, L. R. Carlson, K. Shobatake, M. L. Kowalczyk, and Y. T. Lee, J. Chem. Phys. 72, 1401 (1980).

[11] J. W. Simons, R. J. Paur, H. A. Webster III, and E. J. Bair, J. Chem. Phys. 59, 1203 (1973).

[12] T. Kleindienst and E. J. Bair, Chem. Phys. Lett. 49, 338 (1977).

[13] D. I. Rosen and T. A. Cool, J. Chem. Phys. 62, 466 (1975).

[14] G. A. West, R. E. Weston, Jr., and G. W. Flynn, Chem. Phys. Lett. 56, 429 (1978).

[15] J. F. Riley and R. W. Cahill, J. Chem. Phys. 52, 3297 (1970).

[16] C. J. Hochanadel, J. A. Ghormley, and J. W. Boyle, J. Chem. Phys. 48, 2416 (1968).

[17] T. Kleindienst, J. R. Locker, and E. J. Bair, J. Photochem. 12, 67 (1980).

[18] H. W. Galbraith and J. R. Ackerhalt, in *Laser-Induced Chemical Processes*, edited by J. I. Steinfeld (Plenum, New York, 1981), pp. 1–44; C. D. Cantrell, S. M. Freund, and J. L. Lyman, in *The Laser Handbook*, edited by M. L. Stitch (North-Holland, Amsterdam, 1979), Vol. 3, pp. 485–576.

[19] D. Proch and H. Schröder, Chem. Phys. Lett. 61, 426 (1979).

[20] I. Burak, *J. I. Steinfeld*, and D. G. Sutton, J. Quant. Spectrosc. Radiat. Transfer 9, 959 (1969).

[21] I. Burak, P. L. Houston, D. G. Sutton, and J. I. Steinfeld, IEEE J. Quantum Electron. 7, 73 (1971).

[22] J. I. Steinfeld, I. Burak, D. G. Sutton, and A. V. Nowak, J. Chem. Phys. 52, 5421 (1970).

[23] C. C. Jensen, T. G. Anderson, C. Reiser, and J. I. Steinfeld, J. Chem. Phys. 71, 3648 (1979).

[24] J. Steinfeld, *Molecules and Radiation* (MIT, Cambridge, 1977), p. 27.

[25] J. I. Steinfeld and P. L. Houston, "Double-Resonance Spectroscopy," in *Laser and Coherence Spectroscopy*, edited by J. I. Steinfeld (Plenum, New York, 1978), p. 16.

[26] A. Barbe, 36th Symposium on Molecular Spectroscopy, Ohio State University, Columbus, Ohio, June 15–19, 1981.

[27] A. Barbe, C. Secroun, P. Jouve, N. Monnanteuil, J. C. Depannemaecker, B. Duterage, J. Bellet, and P. Pinson, J. Mol. Spectrosc. 64, 343 (1977).

[28] C. Secroun, A. Barbe, and P. Jouve, *J.* Mol. Spectrosc. 85, 8 (1981).

[29] Only a small number of $T_1:T_2$ measurements have been performed on infrared transitions (Ref. 25). Delayed nutation experiments have indicated that the cross sections for population and phase relaxation are the same for NH_3 (Ref. 30) and CH_3F (Ref. 31). Analysis of the diode–infrared laser-double resonance experiments in SF_6 (Ref. 23) indicates that the cross sections for the two processes do not differ by more than 40%.

[30] G. M. Dobbs, R. H. Micheels, J. I. Steinfeld, J. H-S. Wang, and J. M. Levy, J. Chem. Phys. 63, 1904 (1975).

[31] P. R. Berman, J. M. Levy, and R. G. Brewer, Phys. Rev. A 11, 1668 (1975).

[32] C. Young and R. H. L. Bunner, Appl. Opt. 13, 1438 (1974).

[33] G. K. Moortgat, E. Kudszus, and P. Warneck, J. Chem. Soc. Faraday Trans. 2 73, 1216 (1977).

[34] J. C. Brock and R. T. Watson, Chem. Phys. 46, 477 (1980).

[35] C. L. Lin and W. B. DeMore, J. Photochem. 2, 161 (1973).

[36] S. Kuis, R. Simonaitis, and J. Heicklen, J. Geophys. Res. 80, 1328 (1975).

[37] P. F. Zittel and D. D. Little, J. Chem. Phys. 72, 5900 (1980).

[38] R. Hudson, *Proceedings of the Quadrennial International Ozone Symposium*, edited by J. London (IAMAP, Boulder, 1980), Vol. I, pp. 146–152.

[39] J. C. D. Brand, K. J. Cross, and A. R. Hoy, Can. J. Phys. 56, 327 (1978).

[40] D. H. Katayama, J. Chem. Phys. 71, 815 (1979).

[41] T. D. Padrick, A. K. Hays, and M. A. Palmer, Chem. Phys. Lett. 70, 63 (1980).

CARS Detection of Ozone in Vibrationally Excited States

Since the discovery of the role of vibrationally excited molecules in atmospheric chemistry, the spectroscopic properties and kinetics of such moleclues have attracted much attention. One of the more important molecules in this context is ozone. Vibrationally excited ozone is formed in the stratosphere [1] by the recombination of oxygen

$$O_2 + O + M \rightarrow O_3(v_1,v_2,v_3)$$

The initial population of the various vibrational levels as well as the mechanisms of relaxation to the ground state are still open to speculation.

To study vibrational population distributions requires sensitive detection techniques, as the population of each vibrational level may constitute only a small fraction of the total number of molecules. Recent advances in laser technology have made possible the use of many optical techniques that were unthinkable only a few years ago. Coherent Anti-Stokes Raman Spectroscopy is one such technique [2].

CARS is a third order non-linear optical process which involves two photons of light at frequency ω_1 combining with a photon at ω_2 to produce a fourth coherent photon at the anti-Stokes frequency, $\omega_3=2\omega_1-\omega_2$. The process is greatly enhanced by the presence of a Raman active transition in the medium corresponding to $\omega_1-\omega_2$. It can be shown that the intensity of the CARS signal is proportional to the square of the number density of molecules in the state of lower energy [2]. In this way the intensity of the CARS beam can be used to monitor the population of the various vibrational levels which are Raman active. The advantage of CARS is chiefly its sensitivity. It has been shown [2,6] that the CARS process is inherently several orders of magnitude more sensitive than spontaneous Raman scattering. In practice, the sensitivity of CARS is limited by other third order nonlinear processes. It is usual to split the third order susceptibility into two parts, one that contains the terms which involve CARS and another which includes all other third-order nonlinear processes. These two susceptibilities are referred to as $\chi^{(3)}_{CARS}$ and $\chi^{(3)}_{NR}$, respectively.

The high peak power of Nd:YAG/Dye laser systems lends itself well to CARS. In particular, Valentini [3] has obtained the CARS spectrum of oxygen by using such a laser. The second harmonic of the Nd:YAG at 532 nm is used both as ω_1 and also to pump a dye laser to produce ω_2. The beams impinge on a sample of ozone. Under the intense illumination required the ozone dissociates quite rapidly, and so a spectrum of oxygen was obtained. The lifetime of ozone under these conditions has been estimated to be less than 1 psec.

Recently, the Raman spectrum of ozone has been recorded by using the fourth harmonic of a Nd:YAG laser at 266 nm as a pump [4]. Ozone absorbs strongly at 266 nm [5]. In fact, the absorption coefficient at 266 nm is about ten times the coefficient at 532 nm. The Raman spectrum then is greatly resonance enhanced; this enhancement may be of greater importance than the decrease in ozone concentration due to dissociation. This suggests that it could be possible to observe a CARS spectrum of ozone if the appropriate excitation wavelengths are chosen.

We plan to obtain the CARS signal from ozone by judicious choice of excitation wavelength. The intensity of the CARS beam can then be used as a probe to monitor the vibrational energy distribution. The availability of a high power Nd:YAG/Dye laser allows any of several possible wavelengths. The excitation beam, ω_1, can be 532, 355, or 266 nm, with ω_2 varied appropriately. The Raman spectrum at 266 nm suggests use of this wavelength. The intensity of the CARS beam at the three wavelengths are estimated to be in the ratio $10^4:10^2:1$ if dissociation is not considered. The pressure dependence of the CARS signal is shown in Fig. 1 for the three wavelengths in question. A typical value of $\chi_{NR}^{(3)}$ for gases at one atmosphere is $2.4 \times 10^{-18} cm^3/erg$ [6]. This susceptibility was scaled to one torr and a "signal" calculated for each wavelength. This value is plotted as a short horizontal line along the left side of the graph. These non-resonant photons define the detectivity of ozone in one torr of buffer gas.

To date, a strong CARS signal has been obtained from a low-pressure sample of N_2O gas in a static cell. CARS experiments on both ground-state and vibrationally excited ozone are planned to begin immediately following installation of the required digital signal-averaging equipment in the Spectroscopy Laboratory.

References

1. W.T. Rawlins, G.E. Caledonia, and J.P. Kennealy, J. Geophys. Res., 86. 5247 (1981).
2. S. Druet and J.-P. Taran, in Chemical and Biological Application of Lasers, Vol. IV, C.B. Moore, ed. (Academic Press, New York, 1979) p. 187.
3. J.J. Valentini, D.S. Moore, and D.S. Bomse, in press.
4. D.G. Imre, J.L. Kinsey and R.W. Field, in press.
5. E.C.Y. Inn and Y. Tanaka, J. Opt. Soc., 43, 870 (1953).
6. J.W. Nibler and G.V. Knighten, in Raman Spectroscopy of Gases and Liquids, A. Weber, ed., p. 253-305 (1979).

Fig. 1. The intensity of the CARS signal is plotted vs. ozone pressure for three Nd:YAG wavelengths. The horizontal lines represent the number of photons that would result from the non-resonant part of the third order susceptbility.

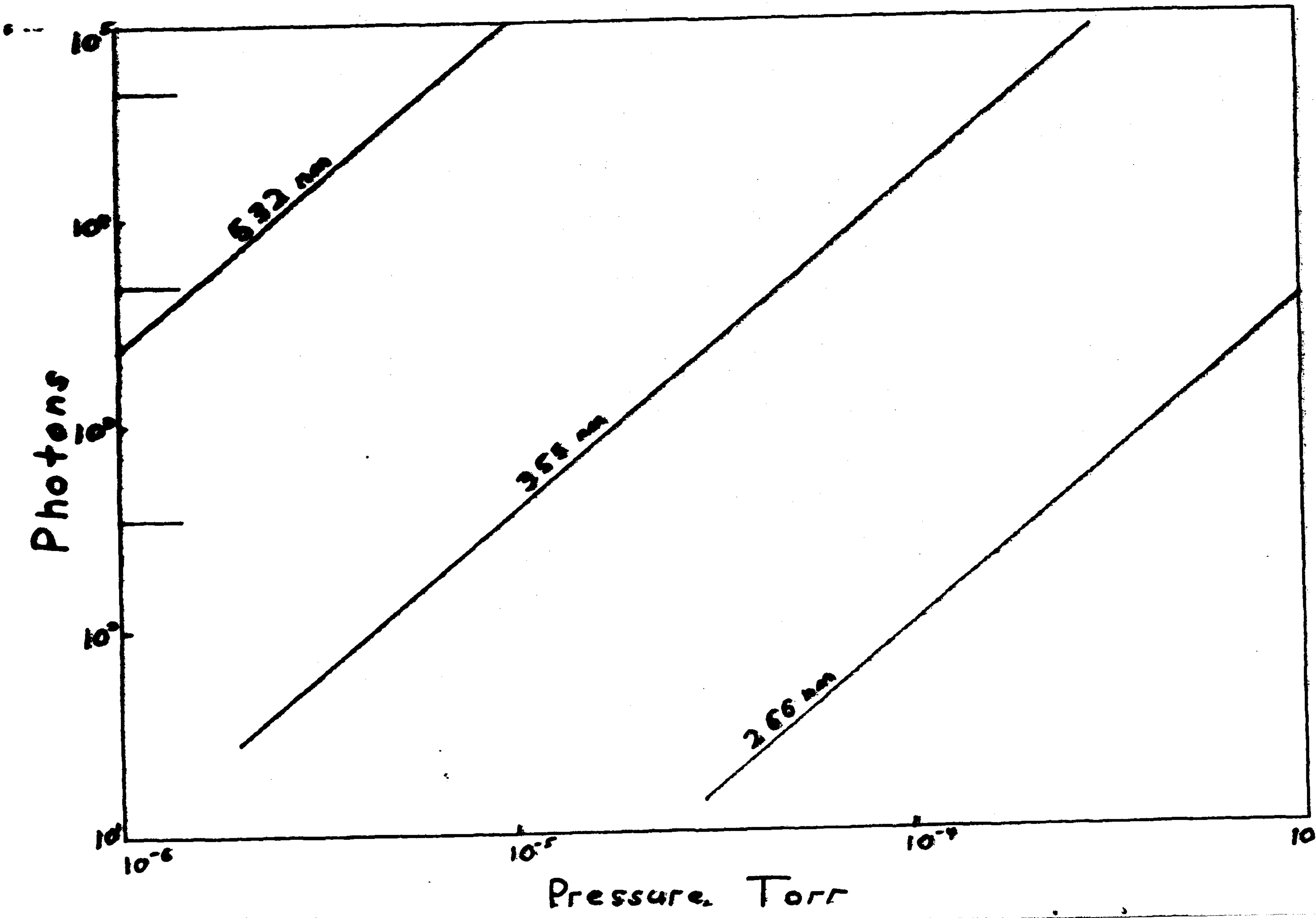

Infrared Emission and Absorption strength for $^{14}N^{15}N$

Dipole radiation from $^{14}N^{15}N$ in the 4.4-μm region has been suggested as making a significant contribution to the infrared luminosity of the upper atmosphere (Gordietz *et al.*, Planet. Space Sci. 26, 933 (1978)). This is based on an assumed Einstein emission coefficient $A_{10} = 0.02 \text{ sec}^{-1}$. We show here that this estimate is almost certainly incorrect, and that the true dipole strength of $^{14}N^{15}N$ must be many orders of magnitude smaller.

Dipole-allowed transitions in homopolar neutral diatomic molecules which are heteronuclear by virtue of isotopic substitution arise from breakdowns of the Born-Oppenheimer separation of electronic and nuclear-vibrational motion. For the best-studied case of HD, the transition moment μ_{10} has been measured to be $5\text{X}10^{-5}$ Debye ($1D = 10^{-18}$ esu·cm) (McKellar, Can. J. Phys. 52, 1144 (1974)). We note the relationship between dipole moment μ_{10} and absorbance,

$$|\mu_{nm}|^2 = \frac{3hc}{8\pi^3 N_o} \; \frac{2J+1}{\binom{J+1}{J} P_J} \; \frac{1}{\rho \ell \nu_o} \int \ell n \; \frac{I_o(\nu)}{I(\nu)} \; d\nu \qquad (1)$$

which can be evaluated numerically (with $R_{nm} = \mu_{nm}/10^{-18}$, ρ in amagat, ℓ in cm, ν_o and $\delta\nu$ in cm^{-1}).

$$|R_{nm}|^2 \simeq (8.94\text{X}10^{-2}) \frac{2\,J+1}{\binom{J+1}{J} P_J} \cdot \frac{1}{\rho \ell \nu_o} \cdot \left(\ell n \; \frac{I_o}{I}\right)_{peak} \cdot \delta\nu \qquad (2)$$

We can also find the A coefficient from

$$A_{10} = \frac{64\pi^4}{3h} \; \frac{|R_{nm}|^2}{\lambda_0^3} = 3\text{X}10^{-7} \left(\frac{1}{\lambda_o}\right)^3 \; |R_{nm}|^2 \qquad (3)$$

with λ_o in cm; $A_{10} = 3.75\text{X}10^{-5} \text{ sec}^{-1}$ for HD (1→0).

The theory of the nuclear-motion-induced dipole transition moment (Bunker, J. Mol. Spectroscopy 46, 119 (1973)). gives

$$\mu_{10} = \mu_{rot}(1,0) + \mu_{elec}(1,0) + \mu^{\alpha}_{vib}(1,0) + \mu^{b}_{vib}(1,0) \qquad (4)$$

The several contributions are generally of varying sign and thus partially cancel; but their overall magnitude is determined by the mass scaling factor

$$(2\mu_{\alpha})^{-1} = (m_a - m_b)/m_a m_b \qquad (5)$$

The ratio of $(\mu_{\alpha})^{-1}$ for $^{14}N^{15}N$ to that for HD is approximately $(5X10^{-3})/(0.5) \approx 10^{-2}$; thus, we would expect R_{10} $(^{14}N^{15}N) \approx (10^{-2})$ $(5X10^{-5}) \approx 5X10^{-7}$ D. This corresponds to an A_{10} value from Eq. (3) of $\approx 1X10^{-9}$ sec^{-1}, not $2X10^{-2}$ as in Gordietz (1978).

Using Eq. (2) with $R = 5X10^{-7}$, ρ=0.2 atm $\approx$ 0.2 amagat, ℓ=20m = $2X10^{3}$ cm, and $\delta\nu(N_2)$ 0.03 cm^{-1}, we calculate an expected peak absorbance, ℓn $(I_o/I) \approx 4X10^{-6}$! As best as we can determine, the limiting sensitivity of the Laser Analytics LS-3 diode spectrometer, using derivative detection, is about 1 part in 10^{3} to 10^{4}; thus, direct observation of $^{14}N^{15}N$ dipole absorptions should be impossible.

The A_{10} coefficient of HD^{+} has been calculated (Bates and Poots, Proc. Phys. Soc. A66, 784 (1953); quoted by Garstang in "Atomic and Molecular Processes" (D.R. Bates, ed.), 1962) as 18 sec^{-1}. Vibration-rotation transitions in HD^{+} have been observed (W.H. Wing et al., Phys. Rev. Letts. 36, 1488 (1976)) in an ion beam experiment under conditions which made it impossible to determine $\mu_{10}(HD^+)$; but the conditions of the experiment required a strongly allowed transition, which is consistent with the preceding estimate. Bates and Poots also give an estimate of $A_{10} \simeq 2X10^{-2}$ sec^{-1} for $^{14}N^{15}N^+$, which was the value taken by Gordietz et al. for $^{14}N^{15}N$; this is incorrect, as we will show.

The dipole operator for charged species is

$$\vec{\mu} = e\left(\frac{m_1 - m_2}{2(m_1 + m_2)} \vec{R} - \vec{z}\right) \tag{6}$$

The first term, which arises only for ionic species, is about 3 orders larger than the second term (in electron coordinate $\vec{z}$), which is however the only term contributing to μ_{10} for neutral species. This accounts for the 7 orders' discrepancy between the value quoted by Gordietz, which is appropriate only to ionic $^{14}N^{15}N^+$, and the estimate made here of $A_{10} \simeq 1X10^{-9}$ sec^{-1} for neutral $^{14}N^{15}N$. Note also that the term in $\vec{z}$ scales as $1/\mu_\alpha \sim (m_1-m_2)/m_1m_2$ (Bunker, 1973), while that in $\vec{R}$ scales as $(m_1-m_2)/(m_1+m_2)$; this is reflected in the $A_{10}\ (^{14}N^{15}N^+)/A_{10}\ (HD^+)$ ratio being $\simeq 10^{-3}$, while for the neutrals, $A_{10}\ (^{14}N^{15}N)/A_{10}\ (HD) \simeq 10^{-4}$. To put it bluntly, Gordietz (1978) made a basic error in assuming $A_{10}\ (^{14}N^{15}N) = A_{10}\ (^{14}N^{15}N^+)$, which invalidates all his conclusions about this source of infrared radiation.

Another possible source of infrared transition strength for homopolar molecules is quadrupole radiation. The $S_1(0)$ quadrupole line of HD was observed by McKellar (1974), from which he derived $\bar{Q}(1,0) \simeq 0.1$ Debye - Å (10^{-26} esu-cm^2). A theoretical estimate

(Cartwright and Dunning, J. Phys. B7, 1776 (1974)) for N_2 gives Q_{zz} (1,0) ≈ 0.05 D-Å, only half of the HD value; thus, the dominant radiation of N_2 in the 4.4-μm region is expected to be quadrupole transitions.

Conclusions

Infrared absorption of $^{14}N^{15}N$ is expected not to be observable with stated experimental conditions (0.2 atm, 20m path length, LS-3 diode laser spectrometer), by roughly two orders of magnitude. If the Gordietz estimate of $A_{10} = 2X10^{-2}$ sec^{-1} had been correct, the absorption coefficient would of course be enormous [$\ell n\ (I_o/I) > 10$ at line center]; but it is so nearly certain to be incorrect that a null result can confidently be predicted. The considerations given above suffice to show that the contribution of $^{14}N^{15}N$ to upper-atmosphere infrared radiance can be neglected.

Publications and Presentations: Contract F19628-80-C0028

S.M. Adler-Golden and J.I. Steinfeld, "Vibrational Energy Transfer in Ozone by Infrared-Ultraviolet Double Resonance", Chem. Phys. Letts. 76, 479 (1980).

S.M. Adler-Golden, "Sum Rules for Molecular Electronic Spectra", Chem. Phys. 64, 421 (1982).

S.M. Adler-Golden, E.L. Schweitzer, and J.I. Steinfeld, "Ultraviolet Continuum Spectroscopy of Vibrationally Excited Ozone", J. Chem. Phys. 76, 2201 (1982).

S.M. Adler-Golden and J.I. Steinfeld, "Kinetics and Hartley Band Spectroscopy of Vibrationally Excited Ozone by Infrared-Ultraviolet Double Resonance Spectroscopy", presented at 36th Symposium on Molecular Structure and Spectra (Columbus, Ohio, June 1981).

S.M. Adler-Golden, "Application of Sum Rules to Molecular Electronic Spectra", presented at 36th Symposium on Molecular Structure and Spectra (Columbus, Ohio, June 1981).

J.I. Steinfeld, "Infrared Luminescence of Chemi-and Photon-Activated Polyatomic Molecules", Final Technical Report, AFGL-TR-82-0267.

Distribution

Air Force Geophysics Laboratory AFGL/OPR-1 Hanscom Air Force Base Bedford, Massachusetts 01731 Mr. Arthur Corman Dr. J.P. Kennealy Dr. R. Armstrong	(4)
Air Force Geophysics Laboratory DCASMA/ACO Hanscom Air Force Base Bedford, Massachusetts 01731	(1)
Massachusetts Institute of Technology Office of Sponsored Programs E19-702 Cambridge, Massachusetts 02139 Mr. T. Duff	(1)